Reviewed Preprint
v1 • November 14, 2025
Not revised

Reviewed Preprint
v2 • June 17, 2026
Revised by authors

For correspondence:
sq38@cornell.edu

* These authors contributed equally

Competing interests: S.-B.Q. is the co-founder of EzraBio Inc. Other authors declare no competing interests.

Funding: See page 26

Reviewing editor: Daniel Arango, Northwestern University, United States

Profiling of terminating ribosomes reveals translational control at stop codons

Longfei Jia[1,3,5], Yuanhui Mao[1,4,*], Saori Uematsu[1], Xinyi Ashley Liu[1], Leiming Dong[1], Leonardo Henrique França de Lima[2], Shu-Bing Qian[1]

[1]Division of Nutritional Sciences, Cornell University, Ithaca, United States • [2]Laboratory of Molecular Modelling and Bioinformatics (LAMMB), Department of Physical and Biological Sciences, Campus Sete Lagoas, Universidade Federal de São João Del Rei, São João Del Rei, Brazil • [3]State Key Laboratory of Reproductive Medicine and Offspring Health, Nanjing Medical University, Nanjing, China • [4]Liangzhu Laboratory, Zhejiang University, Hangzhou, China

eLife Assessment

This manuscript reports on the application of ribosome profiling (EZRA-seq and eRF1-seq) and massively parallel reporter assays (MPRA) to identify and characterize sequence elements that regulate translation termination. The authors conclude that a GA-rich element upstream of stop codons is associated with ribosome pausing during translation termination; in contrast, C-rich sequences upstream of stop codons abolish termination pausing. While the overall findings of this study are **useful** and the identification of GA-rich elements upstream of stop codons is **compelling**, support for several other claims remains **incomplete**. Specifically, the evidence that the MPRA results mirror the ribosome profiling, that a C-rich sequence preceding the stop codon promotes termination slippage in cellular mRNAs, and that Rps26 interferes with mRNA interactions to regulate translation termination would benefit from further support.

https://doi.org/10.7554/eLife.109257.2.sa3

Abstract

Accurate termination of protein synthesis is paramount for the integrity of cellular proteome, yet the dynamics and fidelity of ribosome termination remain poorly understood. Here, we establish a profiling strategy to capture terminating ribosomes in mammalian cells and reveal a substantial heterogeneity in ribosome pausing at individual stop codons. We identify a sequence motif upstream of the stop codon that promotes termination pausing, a finding validated by massively paralleled reporter assays. Unexpectedly, reduced termination pausing increases the likelihood of stop codon slippage, giving rise to proteins with heterogenous C-terminal extensions. Mechanistically, we show that sequence-dependent termination pausing arises from post-decoding mRNA scanning by the 3' end of 18S rRNA. We further uncover tissue-specific patterns of termination pausing that correlates with the stoichiometry of Rps26, which modulates mRNA:rRNA interactions. Together, these results establish termination pausing as a distinct translational signature shaped by mRNA sequence contexts, ribosome heterogeneity, and cell type-specific translational control.

Introduction

Eukaryotic mRNA translation terminates when a stop codon (UAA, UAG, or UGA) enters the ribosomal A site, triggering the coordinated actions of the release factors eRF1 and eRF3 [1]. Structurally mimicking a tRNA, eRF1 mediates stop codon recognition and catalyzes hydrolysis of the peptidyl-tRNA bond, while eRF3 promotes this process in a GTP-dependent manner [2]. In parallel, the ribosome recycling factor ABCE1 facilitates completion of termination by promoting

dissociation of the post-termination ribosome [3,4]. Following Upon release of the nascent polypeptide from the P-site, ABCE1 drives splitting of the 80S ribosome into 60S and 40S subunits, enabling subsequent dissociation of deacylated tRNA and mRNA from the 40S subunit and ensuring efficient recycling of ribosomes and mRNAs.

Although translation termination is generally efficient, the three stop codons exhibit varied efficiencies across individual mRNAs [5]. Notably, UGA – the least efficient stop codon – is also the most frequently used in the human transcriptome. When a stop codon is decoded by a near-cognate tRNA, stop codon readthrough (SCR) occurs, generating protein products with C-terminal extensions [6]. Extensive work has demonstrated that the nucleotide context surrounding the stop codon strongly influences termination fidelity [7,8]. For example, a cytosine at the +4 position enhances SCR, consistent with structural evidence that eRF1 accommodates four nucleotides within the A site [9]. In addition, RNA secondary structures downstream of stop codons can stimulate readthrough, as exemplified by the *kelch* mRNA in *Drosophila* [10]. Such structures have been proposed to induce ribosomes pausing at stop codons, thereby biasing competition toward aminoacyl-tRNA decoding.

Beyond SCR, ribosome pausing at stop codons can also trigger frameshifting, as observed during translation of *OAZ* [11]. Unlike SCR, which preserves the original reading frame, termination-coupled frameshifting produces protein products with heterogeneous C-terminal extensions. Promiscuous translation in 3'UTR has also been documented in cells lacking ABCE1 [12], and terminating ribosomes can undergo undergo reinitiation through bi-directional migration in a sequence-dependent manner [13]. Together, these diverse outcomes underscore the dynamic nature of ribosome behavior o at stop codons and suggest that termination fidelity is tightly coupled to ribosome dynamics. However, very little is known whether individual stop codons exhibit distinct termination kinetics, and if so, what is the underlying mechanism.

Ribosome profiling provides a powerful approach to globally interrogate translation termination across all stop codons in their native sequence contexts [14]. Application of this technique to diverse cell types has revealed that translational readthrough is more widespread in cellular mRNAs than previously appreciated [15]. Intriguingly, readthrough displays marked tissue specificity, occurring at elevated levels in the central nervous system [16,17], whereas tissues such as testis exhibit minimal readthrough [10]. These observations suggest that termination fidelity is governed not only by *cis*-acting mRNA elements but also by *trans*-acting factors that modulate the behavior of terminating ribosomes. The mechanistic basis of such cell type-specific regulation, however, remains poorly understood.

Ribosome stalling at premature termination codons has long been associated with nonsense-mediated mRNA decay [18]. However, this model has been challenged by recent studies reporting comparable ribosome occupancy at premature and normal termination codons [19]. Given that nonsense mutations account for >10% of inherited human diseases, including cystic fibrosis and muscular dystrophy [20], there is strong therapeutic interest in selectively promoting readthrough at premature stop codons while preserving accurate termination at normal stop codons. Achieving this goal requires a deeper understanding of ribosome dynamics and regulatory mechanisms operating at individual termination sites.

Here, by profiling terminating ribosomes in mammalian cells and mouse tissues, we uncover a broad spectrum of termination dynamics across the transcriptome. We show that the dwell time of terminating ribosomes is shaped not only by local sequence context but also by ribosome composition. Unexpectedly, ribosome pausing at stop codons functions as a protective translational checkpoint that restrains ribosome sliding and suppresses aberrant translation into the 3'UTR. Mechanistically, we identify the underlying mechanism by uncovering sequence-dependent interactions between mRNA and rRNA that underlie termination pausing, revealing an unanticipated layer of translational control with important physiological implications.

Results

High-resolution Ribo-seq reveals dynamic features of terminating ribosomes

Ribosome profiling provides a global snapshot of translation by sequencing ribosome-protected mRNA fragments (RPFs) [21]. Relative to the coding sequence (CDS), ribosome footprints accumulate at both start and stop codons. We recently developed Ezra-seq, a high-resolution ribosome profiling method with exceptional 5' end precision [22]. Owing to its superior 3-nt periodicity, Ezra-seq enables sensitive detection of start codon-associated ribosome frameshifting [22]. We reasoned that Ezra-seq would also allow detailed characterization of terminating ribosomes. Indeed, when mRNAs are aligned to their annotated stop codons, we observed sharply defined boundaries of termination-associated footprints (Figure 1A, right panel). Unlike initiating ribosomes, which position the AUG codon in the P site, terminating ribosomes place the stop codon in the A site, as indicated by a prominent 5' end peak at –15 nt relative to the stop codon. Consistent with previous reports [14], terminating ribosomes protected a longer stretch of mRNA (Figure 1A, bottom panel). Compared with elongating ribosomes, terminating ribosomes displayed two distinct footprint populations: long (30 – 31 nt) and short (20 – 23 nt) reads, a feature not observed for initiating ribosomes (Figure 1A, bottom panel). These shorter footprints likely represent terminating ribosomes with an unoccupied A-site.

Closer inspection of stop codon-associated footprints revealed an additional 5' end peak at –12 nt, which became more prominent among shorter reads (Figure 1B). Previous toe-printing assays have shown that eRF1 induces a forward movement of terminating ribosomes, shifting the leading edge from +13 nt to +15 nt [23]. Moreover, single-molecule analyses have identified distinct pre- and post-termination phases catalyzed by eRF1 [24]. Together, these observations suggest that the two 5' end peaks correspond to pre- and post-terminating ribosome states, with the latter likely adopting a rotated conformation. However, we cannot exclude the possibility that a subset of these ribosomes transiently positions the stop codon in the P-site prior to ribosome disassembly.

To probe the kinetics of termination pausing, we performed cycloheximide (CHX) chase experiments in HEK293 cells. CHX stalls elongating ribosomes on mRNAs but does not arrest terminating ribosomes [25]. Whereas a 5 min CHX treatment substantially reduced footprint density at stop codons, a 30 min pre-treatment nearly abolished the stop codon-associated peaks (Figure S1A and S1B). These results indicate that terminating ribosomes undergo transient pausing rather than stable stalling at the stop codon. In line with this notion, we observed little accumulation of upstream ribosomes, suggesting that termination pausing rarely triggers ribosome collisions.

Despite the overall presence of termination pausing, ribosome density at individual stop codons varied over several orders of magnitude. To quantify this variability, we calculated a stop codon pausing index for each mRNA by normalizing read density at the stop codon to average CDS occupancy, thereby accounting for differences in mRNA abundance and translation efficiency (Figure 1C). To identify sequence elements associated with termination pausing, we compared mRNAs with high and low pausing indices. Although no significant motifs were detected downstream of stop codons, a GA-rich motif upstream of the stop codon was strongly enriched among mRNAs exhibiting robust termination pausing ($E = 2.1 \times 10^{-23}$, Figure 1C). These findings indicate that certain coding sequences upstream of the stop codon play a critical role in modulating termination dynamics.

For mRNAs lacking termination pausing, ribosomes may either dissociate i rapidly from the mRNA or undergo stop codon readthrough. These scenarios are expected to produce distinct ribosome occupancy patterns in 3'UTR. Strikingly, we observed higher 3'UTR ribosome density on mRNAs lacking termination pausing (Figure 1D). This effect could not be explained by downstream sequence bias, as the identity of the +4 nt had minimal impact on 3'UTR translation (Figure S1C). Moreover, 3'UTR-associated footprints exhibited poor 3nt periodicity, in sharp contrast to the well-

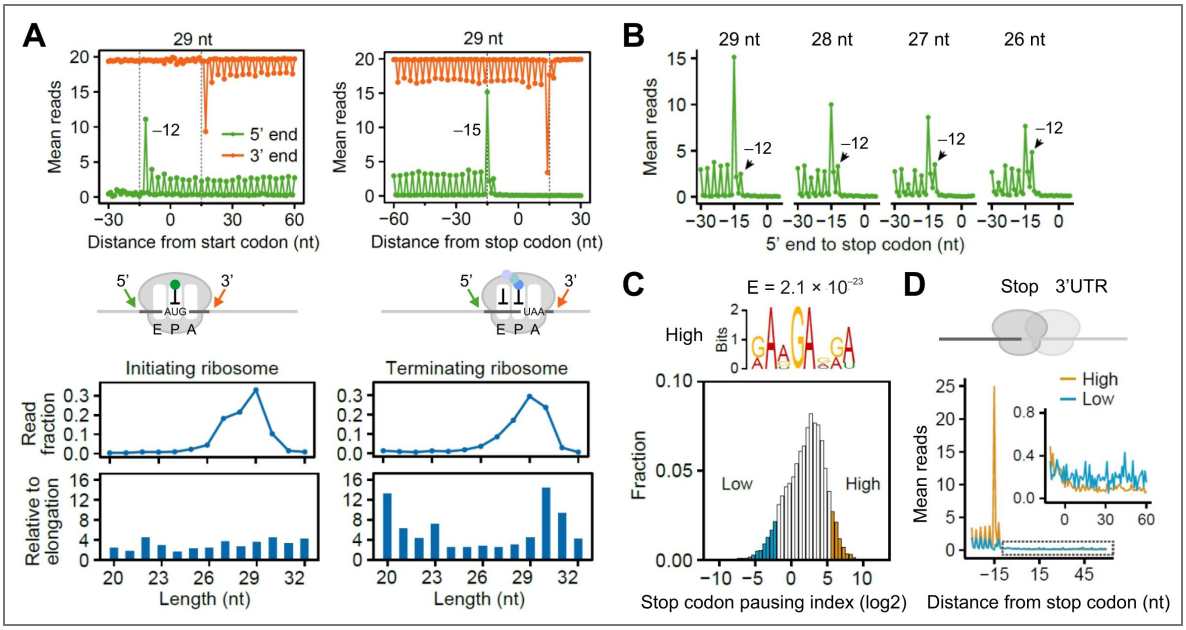

Fig. 1. Characterizing terminating ribosomes using Ribo-seq.

(A) Aggregation plots of mean Ribo-seq reads around the start (left) and stop (right) codons. Both 5′ end (green) and 3′ end (orange) of footprint reads (29 nt) were used for mapping. For bottom panels, the line plots show the distribution of reads with different lengths, whereas the bar plots show the read distribution of initiating (left) and terminating (right) ribosomes relative to elongation ribosomes. **(B)** Aggregation plots of mean Ribo-seq reads around the stop codon. The reads were stratified by the length followed by mapping using the 5′ end of footprint reads. **(C)** A histogram plot of ribosome pausing index at individual stop codon. The top shows the enriched sequence motif of mRNAs with strong ribosome pausing at stop codons. **(D)** Aggregation plots of mean Ribo-seq reads around the stop codon. “High” and “Low” refer to mRNAs with differential pausing indexes shown in (C). The 3′UTR read density was highlighted in the insert.

phased CDS reads (Figure S1D). These observations suggest that canonical stop codon readthrough alone cannot account for the elevated 3'UTR ribosome density observed in the absence of termination pausing.

Profiling of terminating ribosomes by eRF1-seq

To directly interrogate the dynamics of translation termination, we developed a terminating ribosome profiling strategy by isolating ribosomes associated with eRF1 (Figure 2A). HEK293 cells were first crosslinked by formaldehyde, followed by cell lysis and RNase I digestion. Monosomes were isolated by sucrose gradient centrifugation, and eRF1-bound ribosomes were subsequently enriched by immunoprecipitation, as confirmed by immunoblotting (Figure S1E). In the absence of crosslinking, ribosomal proteins were minimally recovered by the eRF1 antibody, consistent with the transient nature of eRF1-ribosome interactions. Deep sequencing of ribosome-protected fragments from eRF1-bound ribosomes (eRF1-seq) revealed a pronounced accumulation of reads precisely at the annotated stop codons (Figure 2A, right panel). Remarkably, eRF1-seq retained single-nucleotide resolution, enabling unambiguous identification of termination sites on endogenous mRNAs (Figure 2B). Similar to conventional Ribo-seq, eRF1-seq also observed the forward-shifted footprints characteristic of post-termination ribosomes (Figure 2C). With excellent reproducibility between biological replicates (Figure S1F), eRF1-seq robustly and selectively profiles terminating ribosomes.

Consistent with our Ribo-seq analyses, eRF1-seq revealed substantial heterogeneity in termination pausing, as not all mRNAs displayed prominent eRF1 peaks at their annotated stop codons (Figure 2B). To identify determinants of this variability, we compared mRNAs with and without eRF1 peaks. Neither 3'UTR length nor downstream sequence features correlated with eRF1 peak height (Figure S1G). In contrast, sequences upstream of the stop codon were significantly enriched for a GA-rich motif among mRNAs exhibiting strong eRF1 peaks (Figure 2D). This observation mirrors the motif identified by Ribo-seq analysis (Figure 1C), reinforcing the conclusion that termination pausing is an intrinsic, sequence-encoded property of individual mRNAs. Notably, all three stop codons exhibited similar pausing features and shared upstream sequence motifs (Figure S1G and S1I).

eRF1-seq reveals alternative termination sites

Despite the prominent peak at annotated stop codons, individual eRF1 peaks were broadly distributed across transcripts, spanning the 5'UTR, CDS, and 3'UTR (Figure 3A). The presence of eRF1 peaks in the 5'UTR is not unexpected, as ~50% of human mRNAs harbor upstream open reading frames (uORFs) [26]. Indeed, ~30% of eRF1 located in the 5'UTR coincided with termination sites of uORFs previously identified by Ribo-seq (Figure S2A). By revealing additional, previously unannotated termination sites in the 5'UTR, eRF1-seq substantially expands the catalog of uORFs. Nearly all A-site codons underlying 5'UTR eRF1 peaks corresponded to canonical stop codons (Figure 3B), and Ribo-seq revealed a reduction in read density downstream of those sites (Figure 3B, right panel), consistent with *bona fide* translation termination. In addition to the 5'UTR, we identified a total of 807 eRF1 peaks in the 3'UTR that shared similar features (Figure S2B). Compared with conventional Ribo-seq, which typically yields sparse 3'UTR reads, eRF1-seq provided an improved signal-to-noise ratio for detecting translation events in the 3'UTR.

Even under stringent peak-calling criteria, eRF1-seq detected a substantial number of peaks within CDS. Many of these CDS-associated eRF1 peaks positioned their A sites at in-frame sense codons (Figure S2C). Notably, the majority of those codons were "stop-like" in that they corresponded to frameshifted versions of canonical stop codons. For example, CUG represents a –1 frameshifted UGA, whereas GAG, GAA, and AAG represent +1 frameshifted UGA or UAA. Despite robust eRF1 occupancy, those sense codons did not trigger translation termination, as Ribo-seq revealed no decrease in downstream read density (Figure S2C). These observations suggest that eRF1 can transiently compete with cognate A-site tRNAs during elongation, resulting in false termination attempts.

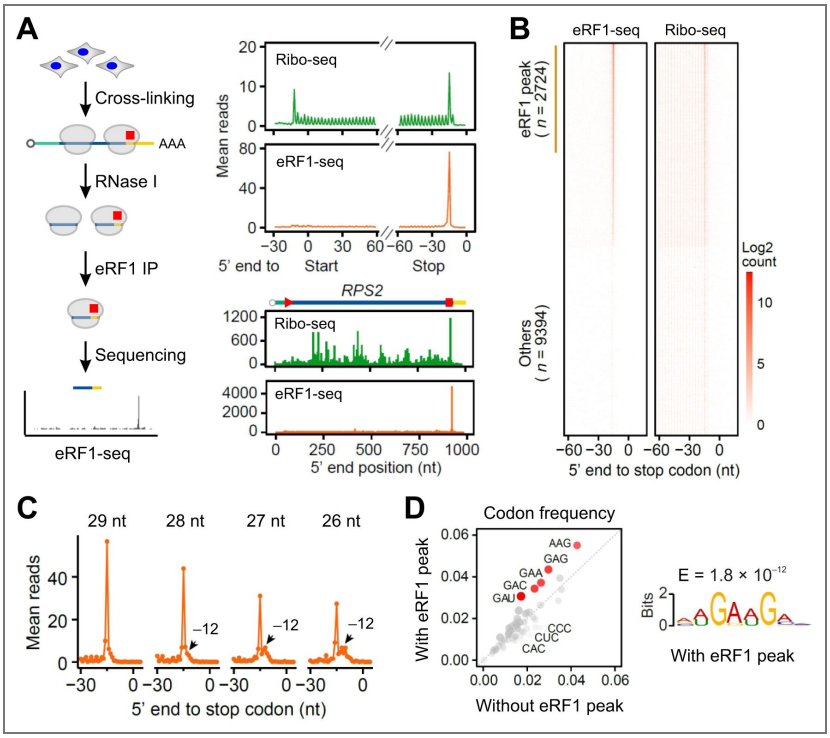

Fig. 2. Characterizing terminating ribosomes using eRF1-seq.

(A) The left panel shows the schematic of eRF1-seq procedures. The right top panel shows the aggregation plots of Ribo-seq (green) and eRF1-seq (orange). The right bottom panel shows a representative mRNA (*RPS2*) with reads obtained from Ribo-seq and eRF1-seq. The 5′ end of reads were used for mapping. **(B)** Heatmaps of individual mRNAs with reads obtained from Ribo-seq (right) and eRF1-seq (left). **(C)** Aggregation plots of mean eRF1-seq reads around the stop codon. The reads were stratified by the length followed by mapping using the 5′ end of footprint reads. **(D)** Comparison of codon frequencies upstream of stop codons between mRNAs with and without eRF1 peaks. The right panel shows the enriched sequence motif for mRNAs with eRF1 peaks at stop codons.

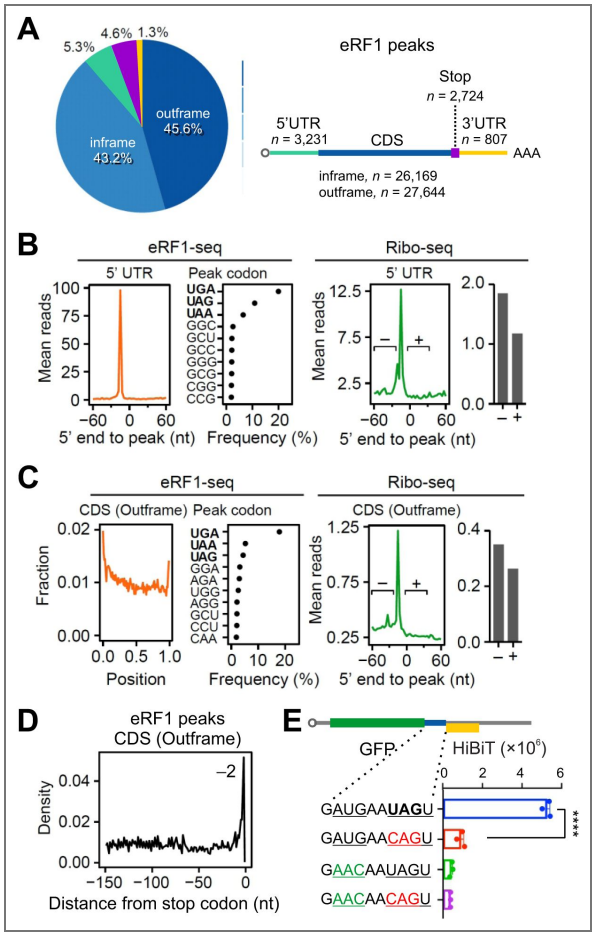

Fig. 3. eRF1-seq reveals prevailing termination sites.

(A) A pie chart shows fractions of eRF1 peaks mapped to different mRNA regions. "Inframe" and "Outframe" refer to the positions of eRF1 peaks within CDS relative to the annotated start codons. **(B)** The left panel shows mean eRF1-seq reads around the position of eRF1 peaks within 5′ UTR. The dot plot shows the frequency of A-site codons at eRF1 peaks. The right panel shows mean Ribo-seq reads around the position of eRF1 peaks within 5′ UTR. The bar graph shows the mean ribosome densities before (-) and after (+) the eRF1 peaks. **(C)** The left panel shows mean eRF1-seq reads around the position of out-of-frame eRF1 peaks within CDS. The dot plot shows the frequency of A-site codons at eRF1 peaks. The right panel shows mean Ribo-seq reads around the position of out-of-frame eRF1 peaks within CDS. The bar graph shows the mean ribosome densities before (-) and after (+) the eRF1 peaks. **(D)** The distribution of eRF1 peaks before the annotated stop codon. Only the out-of-frame eRF1 peaks were used for plotting. **(E)** A bar graph shows the HiBiT-based reporter assays in HEK293-K^{b} cells. HiBiT signals were measured from cells transfected with mRNA reporters bearing different sequences between GFP and HiBiT. Error bars, mean ± s.e.m. $n = 3$ biological replicates. ****$P \leq 0.0001$ by unpaired two-tailed t-test.

In addition to in-frame sense codons, a large fraction of CDS-associated eRF1 peaks corresponded to out-of-frame canonical stop codons, particularly UGA (Figure 3C). Supporting authentic termination at these sites, Ribo-seq revealed reduced ribosome occupancy downstream (Figure 3C, right panel). Interestingly, most out-of-frame termination events occurred near the beginning of CDS. Beyond overlapping uORFs, this pattern further supports the occurrence of start codon-associated ribosome frameshifting that we reported recently [22]. Out-of-frame eRF1 peaks were also enriched near the 3' end of CDS (Figure 3C, 3D), consistent with migration of terminating ribosomes at stop codons to search for upstream start codons (Figure 3D). To directly validate stop codon-associated reinitiation, we inserted a 9 nt sequence derived from *CASQ2*, which contains an out-of-frame AUG codon upstream of a UAG stop codon, between GFP and HiBiT (Figure 3E). Consistent with previous reports [27], mutation of the UAG stop codon abolished reinitiation and eliminated out-of-frame HiBiT expression (Figure 3E), confirming that reinitiation is dependent on termination at the stop codon.

Sequence determinants of termination pausing

Given the wide range of termination pausing observed at individual stop codons, we next thought to identify the sequence determinants of termination pausing using a massively paralleled reporter assay (MPRA). In contrast to analysis of endogenous genes, whose sequences are constrained by evolutionary selection, MPRA leverages fully randomized sequences to enable unbiased identification of sequence elements governing translation behavior. We previously employed a uORF-based MPRA to assess start codon usage with randomized sequence contexts [28]. In this system, mRNA variants with efficient uORF translation are retained in monosome fraction, whereas efficient translation of downstream GFP relocates the mRNA to polysome. Thus, the monosome/polysome ratio serves as a quantitative readout of uORF translation efficiency.

To interrogate stop codon usage, we modified the uORF reporter by replacing the uORF stop codon with a 9-nt randomized sequence (Figure 4A). Introduction of an in-frame stop codon within the insert would terminate uORF translation and restrict the mRNA to the monosome fraction. To eliminate transcriptional variation associated with plasmid-based expression, we synthesized the reporter library by *in vitro* transcription. Following transfection of the mRNA pool into HEK293 cells, monosome and polysome fractions were separated by sucrose gradient centrifugation and analyzed by deep sequencing. Among mRNAs recovered from the monosome fraction, all three canonical stop codons (UGA, UAG, UAA) were strongly enriched (Figure 4A). Importantly, these stop codons were preferentially positioned in-frame within the randomized insert (Figure S3A and S3B). Codons enriched in alternative reading frames were also informative; for example, codons enriched in frame 2 predominantly belong to NUA and NUG, consistent with frameshifted presentations of in-frame stop codons (Figure S3B, bottom panel). Together, these results establish MPRA as a robust platform for dissecting stop codon-associated sequence features.

Ribosomal pausing at uORF stop codons is expected to retain mRNAs in the monosome fraction by suppressing both leaky scanning and stop codon readthrough. We therefore leveraged the monosome/polysome ratio as a proxy for termination pausing. We first examined the impact of downstream sequences by placing a 9-nt randomized sequence immediately after a fixed UAG stop codon (Figure S3C). Despite prior reports that a cytosine (C) at the +4 nt position enhances readthrough [7], mRNA variants containing C-rich downstream sequence were depleted from both monosome and polysome fractions. This depletion likely reflects accelerated mRNA turnover caused by translation into 3'UTR [29,30]. Consistent with our Ribo-seq and eRF1-seq analyses, no specific downstream sequences were enriched in the monosome fraction (Figure S3D), indicating that sequences following the stop codon exert minimal influence on termination pausing.

We next assessed whether upstream sequences modulate stop codon fidelity by inserting a 9-nt randomized sequence immediately before the UAG stop codon (Figure 4B). Strikingly, G-rich sequences were strongly enriched in the monosome fraction (Figure 4B and S3E). Notably, this enrichment lacked reading frame information, indicating that nucleotide composition rather than codon identity governs ribosome pausing at stop codons. In contrast, C-rich sequences were selectively depleted from the monosome fraction (Figure 4B), suggesting that the C-rich

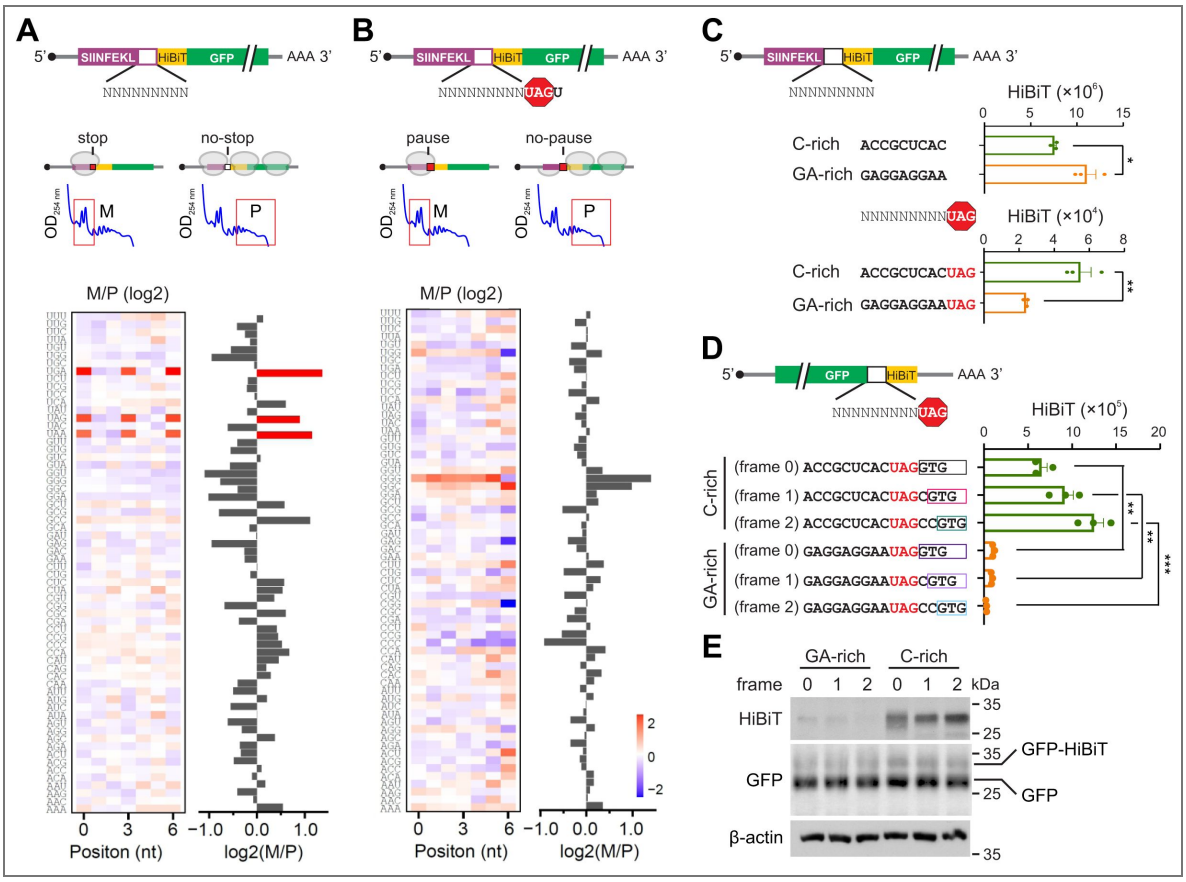

Fig. 4. Termination pausing is influenced by sequence contexts.

(A) The up panel shows the schematic of a massively parallel reporter assay, where the stop codon of uORF was replaced with a random 9-nt sequences. The uORF translation was monitored by the number of associated ribosomes separated by sucrose gradient (M, monosome; P, polysome). The heatmap shows the ratio of monosome fraction over polysome fraction (M/P) when different codons were placed at individual positions within the 9-nt random sequence (left). The stop codons UGA, UAG and UAA are highlighted. The bar graph (right) shows the mean M/P ratio averaged across all positions. **(B)** Similar as (A) except that the random 9-nt sequences were placed before the stop codon UAG. **(C)** Bar graphs show the HiBiT signals in HEK293-K^b cells transfected with mRNA reporters bearing C-rich or GA-rich sequences between the uORF and HiBiT-GFP. The up panel shows the control without the stop codon UAG. Error bars, mean ± s.e.m. $n = 3$ biological replicates. *$P \le 0.05$; **$P \le 0.01$ by unpaired two-tailed t-test. **(D)** A bar graph shows the HiBiT signals in HEK293-K^b cells transfected with mRNA reporters bearing C-rich or GA-rich sequence before the GFP stop codon UAG. The downstream HiBiT sequence was inserted into different reading frames. Error bars, mean ± s.e.m. $n = 3$ biological replicates. **$P \le 0.01$; ***$P \le 0.001$ by unpaired two-tailed t-test. **(E)** Representative Western blots of GFP and HiBiT in HEK293-K^b cells transfected with C-rich or GA-rich reporters as described in (D).

upstream contexts promote sequence stop codon readthrough and downstream translation. These findings closely mirror the sequence dependencies revealed by Ribo-seq and eRF1-seq, reinforcing the conclusion that G-rich sequence intrinsically favor termination pausing.

Stop codon-associated random translation

It was not immediately clear whether translation in the 3'UTR arose from stop codon readthrough or stop codon-associated reinitiation. To distinguish these possibilities, we investigated the nature of downstream translation triggered by upstream C-rich sequences using individual mRNA reporters. Specifically, we placed a C-rich sequence immediately upstream of the uORF stop codon UAG (Figure 4C). Because many C-rich triplets encode proline, an imino acid known to affect ribosome dynamics, we deliberately selected non-proline C-rich codons to avoid confounding effects. As a control, we used a GA-rich sequence identified from eRF1-seq as being associated with strong termination pausing. To sensitively detect translation downstream of the stop codon, we inserted a HiBiT coding sequence immediately after UAG and HiBiT signals can be detected with superior sensitivity [28]. The canonical start codon of HiBiT was omitted to exclude leaky scanning-mediated translation. In the absence of the stop codon, the GA-rich sequence produced higher HiBiT signals than the C-rich sequence, likely reflecting difference in the amino acids encoded by the inserts. Strikingly, in the presence of the UAG stop codon, the C-rich sequence nearly doubled HiBiT signals compared with the GA-rich sequence (Figure 4C, bottom panel). This result is consistent with the MPRA data, indicating that C-rich coding sequences preceding the stop codon not only attenuate termination pausing but also actively promote downstream translation. Importantly, this phenomenon was not restricted to uORFs, as similar results were obtained when the uORF was replaced by a GFP coding sequence (Figure S3F).

Canonical stop codon readthrough is expected to proceed in-frame and generate a fusion protein with a C-terminal extension. To test this model, we placed the HiBiT sequence in different reading frames relative to the stop codon. Unexpectedly, robust HiBiT signals were detected from reporters in both frame 1 and frame 2 (Figure 4D). In contrast, the GA-rich sequence preceding the stop codon strongly suppressed downstream HiBiT translation. This frame-independent effect was reproducible across multiple sequence variants (Figure S3G). To directly examine the translational products, we conducted immunoblotting of whole cell lysates using HiBiT antibodies (Figure 4E). GFP-fusion proteins (~ 30 kDa) were readily detected in C-rich reporters irrespective of the HiBiT reading frames, ruling out reinitiation as the underlying mechanisms. Notably, levels of non-fusion GFP were comparable across reporters, indicating that the differential HiBiT signals were not attributable to altered translation initiation or differences in the amino acids encoded by the upstream inserts. Together, these results demonstrate that C-rich coding sequence promote ribosome sliding at the stop codon, enabling translation into the 3'UTR in all three reading frames.

We next examined the positional dependence of the C-rich effect by introducing C triplets at varying distance upstream of the stop codon. HiBiT reporter assays revealed that a C triplet positioned immediately adjacent to the stop codon was the least effective at promoting 3'UTR translation (Figure S3H). This finding suggests that the sequence determinant governing ribosome sliding resides upstream of the E site, rather than directly at the termination codon itself.

ABCE1 regulates terminating ribosomes independent of the sequence context

ABCE1 (Rli1 in yeast) is a conserved ABC-type protein that plays a crucial role in translation termination and ribosome recycling [3]. Previous studies have shown that depletion of ABCE1 leads to ribosome stalling at stop codons and increased ribosome occupancy within 3'UTRs [12]. To investigate whether ABCE1 exhibits sequence preference towards terminating ribosomes, we knocked down ABCE1 in HEK293 cells using shRNA (Figure S4A). As expected, ABCE1 silencing impaired cell proliferation and reduced global protein synthesis (Figure S4B). We next performed ribosome profiling in ABCE1 KD and control cells using Ezra-seq. After normalizing ribosome occupancy across CDS, loss of ABCE1 resulted in a modest but reproducible increase in ribosome density at stop codons (Figure S4C). Notably, this increase was observed at all three stop codons, an

indication of a global effect. A closer inspection of footprint distribution revealed that ABCE1 depletion selectively increased ribosome density at the –15 nt position, whereas the forward-shifted –12 nt peak was largely unaffected (Figure S4D). These results suggest that ABCE1 primarily facilitates late-stage termination or ribosome splitting, and its absence delays pre-termination progression. A prior study reported that ABCE1 knockdown in HeLa cells promotes translation into 3'UTR in all three reading frames [12]. We were unable to robustly detect this phenomenon by Ribo-seq, likely due to the limited sequencing depth and/or incomplete ABCE1 knockdown in HEK293 cells (Figure S4A). To overcome these limitations, we employed a sensitive HiBiT-based 3'UTR reporter assay, which showed increased 3'UTR translation irrespective of the sequence context upstream of the stop codon (Figure S4E). Therefore, the ribosome recycling factor ABCE1 plays a generic role in translation termination independent of mRNA sequence context.

The 3' end of 18S rRNA influences termination pausing

For a terminating ribosome, the mRNA sequence preceding the stop codon is positioned upstream of the E-site. Given the narrow dimensions of the mRNA channel, it is unlikely that external protein factors such as ABCE1 directly regulate ribosome behavior in a sequence-specific manner. Instead, prior crosslinking studies have shown that mRNA near the exit site interacts with the 3' terminus of 18S rRNA [31]. Such proximity is lso evident in recent cryoEM structures of mammalian initiating ribosomes [32], although stable base pairing was not explicitly resolved (Figure 5A). A similar juxtaposition between mRNA and the 3' end of 18S rRNA has been observed in elongating ribosomes during translocation [33]. Structural modeling based on available cryo-EM data suggests that, from early to late translocation intermediates (POST-1 to POST-3), the distance between the mRNA segment (– 9 to – 3) and the 3' end of 18S rRNA progressively decreases (Figure 5B). These observations support a model in which mRNA undergoes post-decoding scanning by the 3' terminus of 18S rRNA as it exits the ribosome. Notably, the 3' end of 18S rRNA harbors a highly conserved U-rich sequence (GAUCAUUA). We propose that GA-rich mRNA sequences can engage in transient U:A and U:G base pairing with 18S rRNA near the exit site (Figure 5A and S5A), thereby slowing mRNA passage and promoting termination pausing. In contrast, C-rich sequences would evades this rRNA-mediaed checkpoint, resulting in faster mRNA transit and reduced termination pausing.

To directly test whether putative mRNA: rRNA base pairing contributes to termination pausing, we sought to perturb the 3' end sequence of 18S rRNA. Because the presence of hundreds of rDNA copies precludes genome editing approaches such as CRISPR/Cas9, we instead used a previously described 18S rRNA expression system that enables incorporation of exogenously expressed 18S rRNA into ~15% of 40S subunits in transfected cells [34,35]. We engineered an 18S rRNA mutant by substituting the last two U residues with G (GAUCAGGA), a change predicted to weaken interactions with GA-rich mRNA while favoring pairing with C-rich sequence. Overexpression of the mutant 18S in HEK293 cells resulted in polysome profiles comparable to those observed with wild-type 18S rRNA (Figure S5B), and ribosome profiling by Ezra-seq revealed similar ribosome occupancy across coding regions (Figure S5C). However, when mRNAs were stratified by the sequence motif upstream of the stop codon, expression of the mutant 18S reduced the differential termination pausing between GA-rich and C-rich sequences (Figure 5C). Specifically, mRNAs containing GA-rich motifs exhibited reduced stop codon peaks, whereas those bearing C-rich motifs showed increased ribosome accumulation at stop codons. The reciprocal shift in termination pausing in response to mutation of the 18S rRNA 3' end provides strong evidence that sequence-specific termination pausing is mediated by interaction between mRNA and 18S rRNA.

We further validated this model using HiBiT-based reporters to assess 3'UTR translation in cells expressing WT or mutant 18S rRNA. Expression of the mutant 18S rRNA attenuated 3'UTR translation from reporters containing C-rich upstream sequences (Figure 5D). Conversely, reporters bearing GA-rich sequences exhibited increased HiBiT signals, indicative of enhanced 3'UTR translation. Together with the swapped termination pausing profiles observed by ribosome profiling, these results establish a crucial role for the 3' end of 18S rRNA in enforcing termination

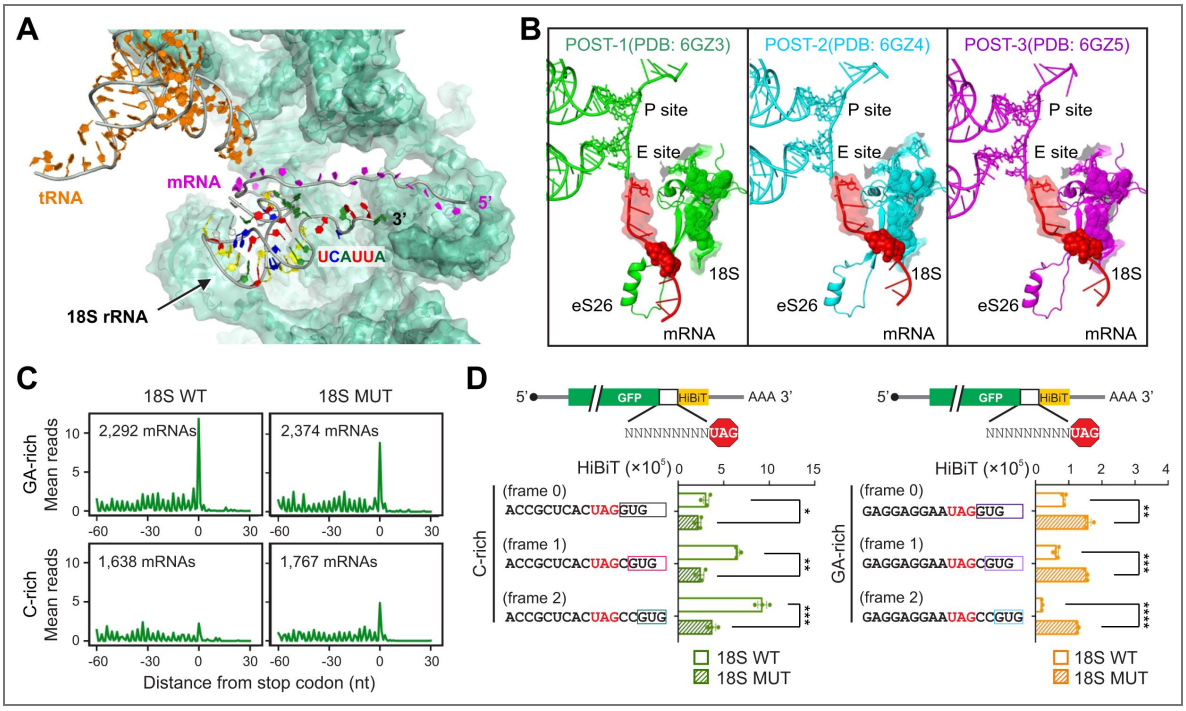

Fig. 5. The 3' end of 18S rRNA influences the dynamic of terminating ribosome.

(A) A cryoEM structures of mammalian initiating ribosomes (PDB: 6ZMW) showing the proximity of the 3' terminus of 18S rRNA and mRNA. **(B)** Superposition of different conformations sampled by normal mode analysis (NMA) of the region mentioned in (A). The analysis was carried out with the mRNA segment from the -10 nt to the +5 nt related to the A-site. The superposition is outlined only for the Rps26 protein (green surface), the mRNA segment (blue surface) and the last 10 nucleotides at the 3' rRNA extremity (dark red surface), with the remaining proteins and rRNA segments at the site described only by the average structure (silver transparent surface and cartoon). The tRNA anticodon loop at the P ribosomal site is shown in dark cyan. **(C)** HEK293 cells were transfected with plasmids encoding 18S rRNA WT or mutant followed by Ribo-seq. Aggregation plots show the mean reads around stop codons of mRNAs with the GA sequence motif or C-rich sequence element. **(D)** HEK293 cells were transfected with plasmids encoding 18S rRNA WT or mutant followed by transfection with mRNA reporters shown in (4D). Bar graphs show the HiBiT signals in transfected cells with HiBiT at different reading frames. Error bars, mean ± s.e.m. n = 3 biological replicates. *$P \le 0.05$; **$P \le 0.01$; ***$P \le 0.001$; ****$P \le 0.0001$ by unpaired two-tailed t-test.

fidelity. Notably, the 3' terminal sequence of 18S rRNA is highly conserved across eukaryotes (Figure S5D). Annotated stop codons in the human genome are preferentially preceded by GA-rich sequences (Figure S5E). In contrast, out-of-frame stop codons show a higher prevalence of C-rich upstream contexts. These patterns suggest an evolutionary advantage for termination pausing at annotated stop codons, likely serving to minimize stop codon slippage and aberrant readthrough while preserving proteome integrity.

Tissue-specific termination pausing

Having established sequence-specific termination pausing in cultured cell lines, we next explored its physiological relevance across tissues. To this end, we conducted Ribo-seq on a diverse panel of mouse tissues, including liver, brain, kidney, heart, and testis (Figure 6A). These tissues displayed distinct polysome profiles and global ribosome occupancy across coding regions (Figure 6A and S6A), reflecting substantial differences in translational states. Strikingly, ribosome density at start and stop codons varied most prominently among tissues and did so in a reciprocal manner. Testis exhibited relatively modest initiation peaks but pronounced ribosome accumulation at stop codons (Figure 6A). In contrast, liver, heart, and brain showed robust initiation peaks with little or no detectable termination pausing. These differences were not attributable to tissue-specific gene expression, as the same reciprocal pattern persisted when analyses were restricted to genes commonly expressed or uniquely expressed in liver and testis (Figure S6B). Consistent with sequence-dependent termination pausing, mRNAs with prominent stop codon peaks in testis were enriched with GA-rich sequences upstream of the stop codon (Figure S6C). Notably, these same mRNAs exhibited minimal termination pausing in liver. Moreover, the attenuated stop codon peak in mouse liver has been independently reported [36], excluding the possibility of technical bias in Ezra-seq.

The unexpected tissue-specific variation in termination pausing points to an additional regulatory layer beyond mRNA sequence context. One candidate is the eukaryote-specific ribosomal protein S26 (Rps26), which contacts mRNA upstream of the E-site [31,37]. Recent cryo-EM structures revealed that both Rps26 (AA62 – 70) and 18S rRNA (nt1857 – 1863) jointly shape the mRNA path near the ribosomal exit site (Figure 5B). Because Rps26 lies between the mRNA and the 3' end of 18S rRNA, its absence could enhance mRNA: rRNA interactions and thereby strengthen termination pausing. Supporting this notion, a recent study demonstrated that Rps26 can dissociate from fully assembled 80S ribosomes under stress conditions, generating ribosome heterogeneity [38]. To assess whether Rps26 abundance varies across tissues, we compared ribosomal proteins in tissue homogenates. When normalized to β-actin, core ribosomal proteins such as Rpl4 were present at comparable levels across tissues, whereas Rps26 levels were markedly reduced in testis relative to other tissues examined (Figure 6B). Differential Rps26 expression between liver and testis is also evident in Human Protein Atlas (*proteinatlas.org*) [39]. We further examined Rps26 distribution across polysome fractions in liver and testis. In liver, Rps26 and the control ribosomal protein RACK1exhibited similar polysome association. In contrast, testis showed pronounced depletion of Rps26 from polysomes (Figure 6C), accompanied by accumulation of Rps26 in ribosome-free fractions. Whether this reflects active dissociation of Rps26 from translating ribosomes in testis remains to be determined. These findings nevertheless suggest Rps26 stoichiometry contributes to tissue-specific termination pausing, likely by modulating access of the mRNA to the 3' end of 18S rRNA.

Rps26 modulates termination pausing

Based on available ribosome structures containing bound mRNA, Rps26 is positioned between the exiting mRNA and the 3' end of 18S rRNA (Figure 7A). We hypothesize that loss of Rps26 would increase the accessibility of the mRNA to the 3' terminus of 18S rRNA, thereby facilitating mRNA:rRNA interactions and promoting termination pausing. Consistent with this model, normal mode analysis (NMA) using anisotropic network models predicts that removal of Rps26 permits coordinated twisting and closer approximate between the mRNA segment (–3 to – 9) and the 3' end

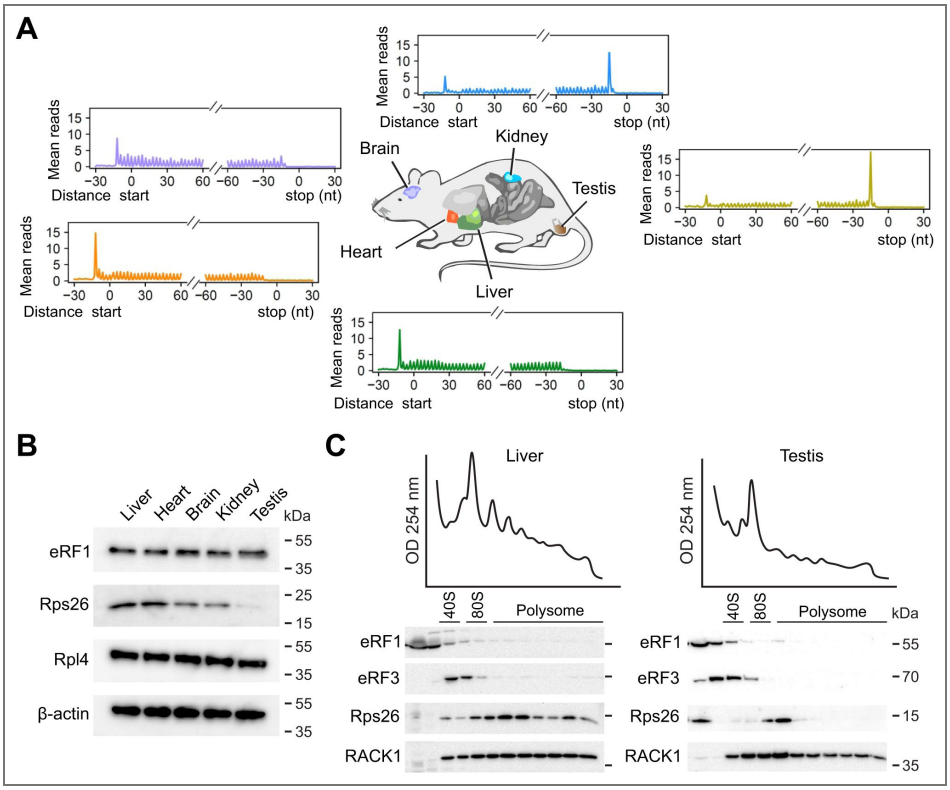

Fig. 6. Differential termination pausing in mouse tissues.

(A) Different mouse tissues were collected followed by Ribo-seq. Metagene analysis shows the distribution of mean ribosome reads across the transcriptome aligned to start and stop codons. **(B)** Representative Western blots of different mouse tissues using antibodies indicated. The experiment was independently repeated three times with similar results. **(C)** Mouse liver and testis were subjected to polysome profiling using sucrose gradient. Representative Western blots of ribosome fractions were conducted using antibodies indicated. The experiment was independently repeated three times with similar results.

of 18S rRNA (Figure 7B). This enhanced spatial parity would be further stabilized when the mRNA sequence is complementary to the rRNA. Given the U-rich nature of the 18S rRNA 3' end, such interactions are predicted to be most favorable for GA-rich mRNA sequences.

To test whether reduced Rps26 levels affect ribosome dynamics at stop codons, we depleted Rps26 in HEK293 cells using shRNA (Figure S7A). Rps26 silencing led to an increased 60S peak and reduced polysome formation (Figure S7B), consistent with its known role in 40S subunit maturation [40]. We then conducted ribosome profiling in parallel with RNA-seq. Remarkably, Rps26 depletion resulted in reduced ribosome density at start codons but increased ribosome accumulation at stop codons (Figure S7C). This reciprocal change mirrors the tissue-specific differences observed between initiation and termination (Figure 6A). Importantly, the elevated termination pausing occurred predominantly at stop codons preceded with GA-rich sequences (Figure 7C). To assess the functional consequences of altered termination dynamics, we employed HiBiT-based 3'UTR reporter assay. Because Rps26 silencing globally reduced protein synthesis (Figure S7B), HiBiT signals were normalized to upstream GFP expression. Under these conditions, only reporters containing GA-rich sequences, but not C-rich sequences, exhibited reduced HiBiT translation in Rps26-depleted cells (Figure 7D). Therefore, Rps26 specifically modulates termination fidelity at GA-rich stop codons by constraining mRNA:rRNA interactions.

To further substantiate this conclusion, we overexpressed Rps26 in HEK293 cells (Figure S7D), which did not perturb polysome formation (Figure S7E). Ribosome profiling revealed that Rps26 overexpression lowered ribosome occupancy from initiation through termination (Figure S7F). When mRNAs are stratified by upstream sequence context, Rps26 overexpression ocaused a pronounced (>50%) reduction in ribosome density at stop codons preceded by GA-rich sequences (Figure 7E). Notably, ribosome density upstream of these stop codons were also diminished, suggesting that increased Rps26 levels broadly restrain mRNA:rRNA engagement during elongation. In contrast, mRNAs harboring the C-rich sequence upstream of the stop codon displayed relatively enhanced termination peaks. To directly link stop codon pausing with termination fidelity, we conducted HiBiT reporter assays t in cells with Rps26 overexpression. In line with reduced termination pausing, Rps26 overexpression increased 3'UTR translation (Figure 7F), confirming that diminished mRNA:rRNA interaction compromises termination fidelity. Collectively, these results establish Rps26 as a key modulator of sequence-specific termination pausing.

Discussion

Translation termination is intrinsically slower than elongation, and stop codons therefore frequently serve as ribosome pausing sites. Insufficient pausing at stop codons can lead to incomplete ribosome dissociation, allowing ribosomes to continue translating into the 3'UTR. Conversely, excessive pausing would delay ribosome recycling and increase the risk of ribosome collisions. Thus, ribosome dwell time at stop codons must be precisely calibrated to balance termination efficiency and fidelity. Since the advent of ribosome profiling, elevated ribosome density at both start and stop codons has been a consistent feature of metagene analyses. However, little has been known about the variability of termination pausing at individual stop codons, let alone the underlying mechanism. By combining high-resolution ribosome profiling [22] with a specialized eRF1-seq approach, we quantitatively defined stop codon pausing indices and uncovered a previously unappreciated role of mRNA sequence context in shaping the dynamics of terminating ribosomes. Unexpectedly, it is the sequence upstream of the stop codon – rather than the stop codon itself or downstream elements – that determine termination pausing. A GA-rich sequence element promotes ribosome pausing, a finding independently confirmed by massively paralleled reporter assay. In contrast, C-rich sequences upstream of stop codons abolish termination pausing. Importantly, loss of termination pausing does not simply result in canonical stop codon readthrough; instead, it triggers stop codon-associated random translation into the 3' UTR, generating proteins with mixed C-terminal extensions. This phenomenon reveals a distinct and more complex mode of termination than classical readthrough.

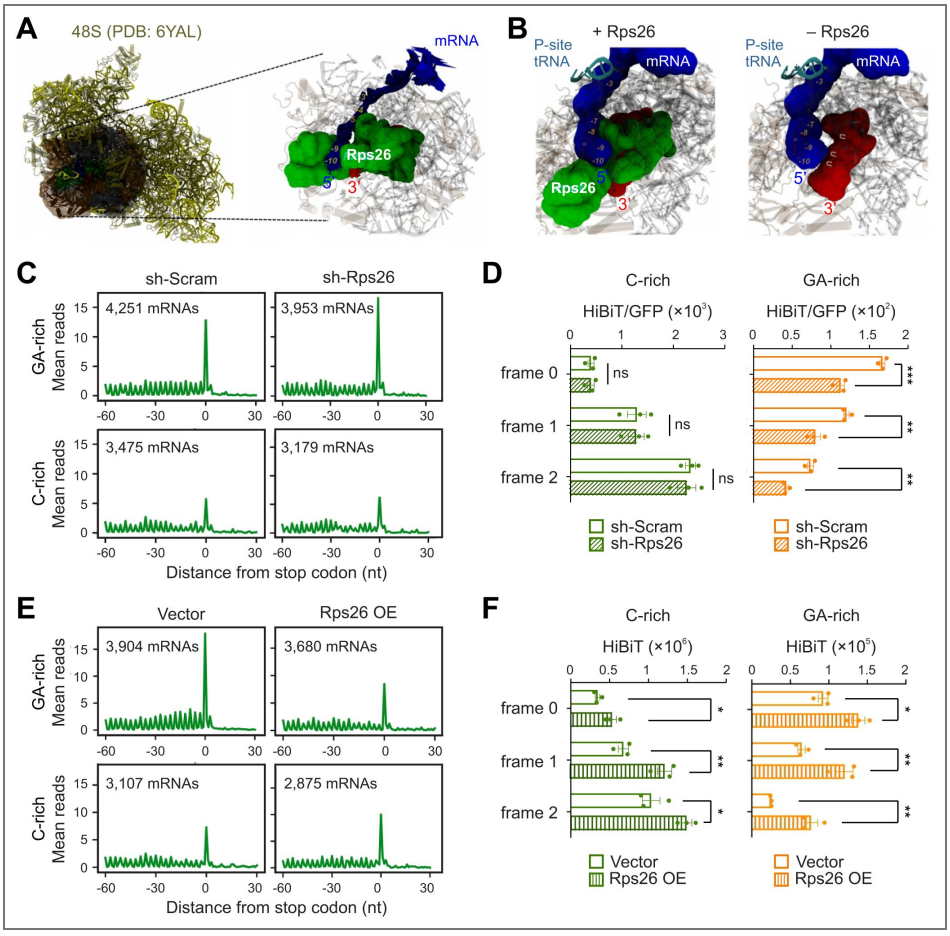

Fig. 7. Rps26 modulates termination pausing.

(A) A cryo-EM structure of the human 48S pre-initiation complex (PDB: 6YAL) depicted in cartoon and colored in yellow. The region at the 5′ exit of the mRNA tunnel centered in Rps26 and extended around 30 Å of this protein is highlighted in transparent surface and in dark colors. **(B)** Conformational sampling by normal mode analysis (NMA) of the region mentioned in (A). The analysis was carried out with the mRNA segment from the -10 nt related to the P-site to the +5 nt related to the A-site. The superposition is outlined only for the Rps26 protein (green surface), the mRNA segment (blue cartoon) and the last 10 nucleotides at the 3′ rRNA extremity (dark red cartoon), with the remaining proteins and rRNA segments at the site described only by the average structure (silver transparent surface and cartoon). The tRNA anticodon loop at the P ribosomal site is omitted on the image. **(C)** HEK293 cells with or without Rps26 knockdown were subjected to Ribo-seq. Aggregation plots show the mean reads around stop codons of mRNAs with the GA sequence motif or C-rich sequence element. **(D)** HEK293 cells with or without Rps26 knockdown were transfected with mRNA reporters shown in 4D. Bar graph shows the HiBiT signals at different reading frames upon normalization to upstream GFP levels Error bars, mean ± s.e.m. $n = 3$ biological replicates. ns, nonsignificant; $^{**}P \leq 0.01$; $^{***}P \leq 0.001$ by unpaired two-tailed t-test. **(E)** HEK293 cells with or without Rps26 overexpression were subjected to Ribo-seq. Aggregation plots show the mean reads around stop codons of mRNAs with the GA sequence motif or C-rich sequence element. **(F)** HEK293 cells with or without Rps26 overexpression were transfected with mRNA reporters shown in 4(D). Bar graph shows the HiBiT signals at different reading frames. Error bars, mean ± s.e.m. $n = 3$ biological replicates. $^{*}P \leq 0.05$; $^{**}P \leq 0.01$ by unpaired two-tailed t-test.

A potential caveat in interpreting sequence-specific termination control is that different nucleotides sequences encode different amino acids, which could independently influence ribosome dynamics. This concern is particularly relevant for C-rich sequences, which often encode proline. However, multiple lines of evidence support the conclusion that nucleotide sequence – not amino acid identity – governs termination pausing. First, the positional effects of sequence elements do not conform to codon triplet boundaries. Second, although proline codons are decoded slowly, C-rich sequences reduce rather than enhance termination pausing. Third, C-rich sequence-promoted downstream translation persists even when proline codons are excluded. Fourth, fusion protein analyses reveal minimal effects of the encoded amino acids on translation outcomes. Fifth, unbiased MPRA analyses identify enrich sequence motifs across all reading frames. These findings collectively demonstrate that mRNA sequences, rather than the encoded peptides, control ribosome behavior at stop codons.

Because the mRNA segment upstream of the stop codon resides near the exit site of the ribosomal mRNA channel, our findings suggest that ribosome - mRNA communication extends beyond the decoding center. Such post-decoding interactions are well established during translation initiation, exemplified by the Shine-Dalgarno (SD) sequence that pairs with the 3' end of 16S rRNA in prokaryotic cells [41]. In eukaryotic cells, analogous base-pairing interactions involving the 3' end of 18S rRNA has been documented in cap-independent translation and cap-dependent translation of histone H4 mRNA [42–44]. We previously reported that the highly conserved 3' terminus of 18S rRNA contributes to elongation pausing via base pairing with certain codons [35]. Our current work extends this principle to translation termination, demonstrating that post-decoding mRNA:rRNA interactions near the exit channel modulate ribosome dwell time at stop codons.

Although ribosomal structures have been solved at near-atomic levels, relatively few contain well-resolved mRNA, owing to its intrinsic flexibility. Crosslinking studies have indicated proximity between mRNA and rRNA near the exit site [31], yet the functional relevance of this interaction remained unclear. Using targeted mutations of the 18S rRNA, we showed that U-rich sequence at its 3' end is crucial for stabilizing mRNAs bearing GA-rich sequence motifs. The involvement of G:U base pairs is particularly notable, as these non-canonical interactions possess unique chemical properties distinct from A:U pairing [45]. Mutation of the U-rich sequence to G reverses termination pausing preferences, shifting pausing from GA-rich to C-rich mRNAs. These results support a model in which mRNA:rRNA base pairing near the exit channel delays mRNA movement following decoding. For terminating ribosomes, the extended dwell time likely enhances eRF1 recruitment, peptide release, and efficient ribosome recycling.

While post-decoding mRNA:rRNA interactions explain sequence-specific termination pausing, they do not fully account for tissue-specific differences we observed. Termination pausing is particularly strong in testis, a tissue characterized by exceptional transcriptomic diversity arising from promiscuous transcription [46] and attenuated nonsense-mediated decay [47]. Testis translation also displays unique features, including reduced dependency on codon optimality [48] and coupling of 3'UTR translation to piRNA biogenesis [49]. In this context, heterogenous ribosome dwell times at stop codons may facilitate functional partitioning of ribosomes beyond annotated coding regions. Whether termination dynamics are developmentally regulated during spermatogenesis remains an important question for future study.

To identify cell type-specific regulators of termination pausing, we focused on the eukaryotic-specific ribosomal protein Rps26. Like the 3' end of 18S rRNA, Rps26 crosslinks to mRNA regions upstream of the P-site [31,37], and occupies a strategic position beneath the mRNA segment upstream of the E-site, effectively shielding it from direct interaction with 18S rRNA (Figure 7A). Loss of Rps26 enhances termination pausing at GA-rich stop codons, whereas Rps26 overexpression dampens pausing, consistent with a model in which Rps26 restricts mRNA:rRNA base pairing. Intriguingly, Rps26 was previously shown to regulate initiation by recognizing Kozak sequence elements [50]. The consensus vertebrate Kozak context (GCCRCCAUGG) highlights the importance of purine at key positions, paralleling our observations at stop codons. The reciprocal changes in initiation and termination peaks upon Rps26 depletion suggest that coordinated mRNA:rRNA:Rps26 interactions operate throughout the translation cycle.

Perhaps the most expected finding of our study is that tissue-specific termination pausing is governed by Rps26 stoichiometry. In yeast, Rps26 can dissociate from fully assembled 80S ribosomes under stress [38], raising the possibility that mammalian ribosomes similarly exist in Rps26-variable states. is either sub-stoichiometric or loosely integrated into the 80S ribosomes. Notably, Rps26 haploinsufficiency is linked to Diamond-Blackfan anemia (DBA) [51]. Prolonged termination pausing and impaired ribosome recycling may contribute to the hematologic defects observed in DBA, particularly given the high reliance of erythroid cells on ribosome rescue pathways and their elevated levels of 3'UTR translation [52]. A deeper understanding of stop codon-associated translational quality control may therefore open new avenues for therapeutic interventions in DBA and other diseases caused by premature termination of nonsense mutations.

Methods

Materials availability

Reagents and materials produced in this study are available from the Lead Contact pending a completed Materials Transfer Agreement.

Experimental model and subject details

Cell lines

HEK293-K^b cells and Lenti-X 293T cells are maintained in Dulbecco's Modification of Eagle's Medium (Corning, 10-013-CV) with 10% fetal bovine serum (Sigma, 12306C). All cells were grown at 37°C with 5% CO_2.

Mouse strains

C57BL/6 mice were obtained from the Jackson laboratory. All animals (1-6 mice per cage) were housed in a 12 h light/dark cycle in the Weill Hall animal facility at Cornell University with the supervision of the Center for Animal Resources and Education (CARE) breeding program. All animals used in this study were handled in accordance with federal and institutional guidelines, under a protocol approved by the Cornell University Institutional Animal Care and Use Committee, protocol 2017-0035. Mice were housed under specific pathogen-free conditions in an Association for the Assessment and Accreditation of Laboratory Animal Care International-accredited facility and cared for in compliance with the Guide for the Care and Use of Laboratory Animals.

Method details

Antibodies

The following antibodies were used at their indicated experimental concentrations: anti-GFP (Proteintech, 50430-2-AP, 1:1000), anti-eRF1 (Santa Cruz Biotechnology, sc-365686, 1:200), anti-eRF3 (Santa Cruz Biotechnology, sc-515615, 1:200), anti-Rps26 (Proteintech, 14909-1-AP, 1:500), anti-Rpl4 (Proteintech, 11302-1-AP, 1:1000), anti-ABCE1 (Abcam, ab185548, 1:1000), anti-myc (Cell Signaling, 2272S, 1:1000), anti-RACK1 (BD Transduction Laboratories, 610177, 1:1000) and anti-β-Actin ((Sigma-Aldrich, A5441, 1:5,000). anti-mouse IgG horseradish peroxidase (HRP)-conjugated secondary antibodi (Sigma-Aldrich, A0168, 1:10,000) or anti-rabbit IgG secondary antibody conjugated to peroxidase (Sigma-Aldrich, A9169, 1:10,000).

Plasmid construction

The template of EGFP-HiBiT reporters were PCR-amplified from the pcDNA3-EGFP vectors using reverse primer containing the desired sequence. In some cases, the template of reporters based on HiBiT-EGFP were generated using a two-step PCR amplification approach. First, the full length of HiBiT and EGFP was amplified from pcDNA3-EGFP to generate HiBiT-EGFP. The resulting PCR product was used as a template to produce the full-length reporter using a second forward primer containing the respective sequence. After column purification (QIAGEN), the DNA template (1~2 μg) was utilized to generate mRNAs suitable for transfection. For exogenous Rps26, the full-length coding sequence of human Rps26 was cloned into pcDNA3.1(myc-His B) using BamH I and Hind III

REAGENT or RESOURCE	SOURCE	IDENTIFIER
Antibodies		
Anti-GFP antibody	Proteintech	Cat# 50430-2-AP; RRID: AB_11042881
Anti-eRF1 antibody	Santa Cruz Biotechnology	Cat# sc-365686; RRID: AB_10843214
Anti-eRF3 antibody	Santa Cruz Biotechnology	Cat# sc-515615
Anti-Rps26 antibody	Proteintech	Cat# 14909-1-AP; RRID: AB_2180361
Anti-Rpl4 antibody	Proteintech	Cat# 11302-1-AP; RRID: AB_2181909
Anti-ABCE1 antibody	Abcam	Cat# ab185548; RRID: AB_2858278
Anti-myc antibody	Cell Signaling	Cat# 2272S
Anti-RACK1 antibody	BD Transduction Laboratories	Cat# 610177; RRID: AB_397576
Anti-β-Actin antibody	Millipore Sigma	Cat# A5441; RRID: AB_476744
Anti-Mouse IgG (Fc specific)-Peroxidase antibody	Millipore Sigma	Cat# A0168; RRID: AB_257867
Anti-Rabbit IgG (whole molecule)-Peroxidase antibody	Millipore Sigma	Cat# A9169; RRID: AB_258434
Bacterial and virus strains		
DECIPHER pRSI9-U6-(sh)-UbiC-TagRFP-2A-Puro	Cellecta	N/A
Subcloning Efficiency DH5a Competent Cells	Thermo Fisher Scientific	Cat# 18265-017
Chemicals, peptides, and recombinant proteins		
Dulbecco's Modified Eagle Medium	Corning	Cat# 10-013-CV
Fetal bovine serum	Millipore Sigma	Cat# 12306C-500ML
Opti-MEM I Reduced Serum Medium	Thermo Fisher Scientific	Cat# 31985-070
Dulbecco's Phosphate Buffered Saline	Thermo Fisher Scientific	Cat# 14190250
BamHI-HF	New England BioLabs	Cat# R3136S
HindIII-HF	New England BioLabs	Cat# R3104S
Lipofectamine MessengerMAX	Invitrogen	Cat# LMRNA015
Lipofectamine 2000	Invitrogen	Cat# 11668-500
DL-Dithiothreitol	Millipore Sigma	Cat# D0632-5G
Blotting-Grade Blocker	Bio-Rad	Cat# 1706404
Tween-20	Millipore Sigma	Cat# P7949-500ML
Triton-X100	Millipore Sigma	Cat# T9284-100mL
EDTA-free Protease Inhibitor Cocktail Tablets	Millipore Sigma	Cat# 11 836 170 001
Puromycin	Millipore Sigma	Cat# P7255
Cycloheximide	Millipore Sigma	Cat# C1988-1G
TRIzol LS Reagent	Invitrogen	Cat# 10296-028
Nuclease-Free Water	Invitrogen	Cat# AM9932
SUPERase·In RNase Inhibitor	Invitrogen	Cat# AM2696
RNase I	Invitrogen	Cat# AM2295
15% TBE-Urea Gels	Invitrogen	Cat# EC6885BOX

Key resources table.

SYBR Gold nucleic acid gel stain	Invitrogen	Cat# S-11494
Sodium acetate buffer solution	Millipore Sigma	Cat# S7899-500ML
T4 Polynucleotide Kinase	New England BioLabs	Cat# M0201L
E. coli Poly(A) Polymerase	New England BioLabs	Cat# M0276L
T4 RNA Ligase 2, truncated	New England BioLabs	Cat# M0242L
Ezra enzyme	This paper	N/A
UltraPure™ SSC, 20X	Invitrogen	Cat# 15557044
Streptavidin Magnetic Beads	New England BioLabs	Cat# S1420S
RNaseOUT Recombinant Ribonuclease Inhibitor	Invitrogen	Cat# 10777-019
8% TBE Gel	Invitrogen	Cat# EC6215BOX
Pierce Protein A/G Agarose	Thermo Fisher Scientific	Cat# 20421
Critical commercial assays		
QIAquick Gel Extraction Kit	Qiagen	Cat# 28706
Q5 Site-Directed Mutagenesis Kit	New England BioLabs	Cat# E0554S
mMESSAGE mMACHINE T7 Transcription Kit	Invitrogen	Cat# AM1344
Poly(A) Tailing Kit	Invitrogen	Cat# AM1350
RNA Clean and Concentrator-25 Kit	Zymo	Cat# R1018
Nano-Glo HiBiT Lytic Detection System	Promega	Cat# N3040
Nano-Glo HiBiT Blotting System	Promega	Cat# N2410
SuperScript III Reverse Transcriptase	Thermo Fisher Scientific	Cat#18080-044
Deposited data		
Raw and analyzed data	This paper	GEO:
Experimental models: Cell lines		
Human: HEK293-K[b]	Laboratory of Jonathan Yewdell	N/A
Human: Lenti-X 293T	Takara Bio	Cat# 632180
Experimental models: Organisms/strains		
Mouse: C57BL/6	Jackson Laboratory	N/A
Oligonucleotides		
Oligonucleotide sequences used in this study are provided in Table S1	This paper	N/A
Recombinant DNA		
pcDNA3.1 (myc-His B)-Rps26	This paper	N/A
pRL-CMV-18S rRNA wild type	Burman and Mauro, 2012	N/A
pRL-CMV-18S rRNA mutant	This paper	N/A
Software and algorithms		
GraphPad Prism	Dotmatics	RRID: SCR_002798
Snapgene	Dotmatics	RRID: SCR_015052
R	The R Project	https://www.r-project.org/
Custom Code	This paper	

Key resources table. (continued)

restriction sites. To create the 18S rRNA mutant, site-directed mutagenesis was performed using Q5 Site-Directed Mutagenesis Kit (New England Biolabs) according to the manufacturer manual. Mutation was confirmed by Sanger DNA sequencing. DNA sequences of all primers used in this study are listed in the Key Resources Table.

In vitro transcription

To prepare mRNA reporters, 1~2 μg PCR products described above were utilized as templates to generate mRNAs suitable for transfection. In vitro transcription was performed for 1 h at 37 °C using mMESSAGE mMACHINE T7 Transcription Kit (Invitrogen) followed by poly(A) tailing (Ambion) at 37 °C for 30 min. The resulting RNAs were purified using RNA Clean & Concentrator (Zymo Research) following the manufacturer's instruction and stored at -80 °C.

Transfection

For mRNA reporter transfection, cells were transfected with in vitro transcribed mRNA (1 μg) in Opti-MEM (125 μl) using Lipofectamine MessengerMAX (1 μl) in Opti-MEM (125 μl), unless stated otherwise. The cells were incubated with the mRNA/Lipofectamine MessengerMAX mixture for 4 h followed by immunoblotting, HiBiT assay or polysome profiling. For Rps26 or 18S rRNA overexpression, 2 μg plasmids were mixed with 4 μl Lipofectamine 2000 (Invitrogen) followed by incubation with cells for at least 24 h, unless stated otherwise.

HiBiT assay

Cells grown in a 35 mm dish were transfected with mRNA reporters (1 μg) described above. Transfected cells were washed with PBS and then lysed using a Nano-Glo HiBiT Lytic Detection System (Promega) according to manufacturer's instructions. HiBiT signals were measured using Luminometer (Atto).

Immunoblotting

Cells grown in a 6-well plate were transfected with transcribed mRNA reporters (1 μg) described above. Transfected cells were washed twice with ice-cold PBS and lysed on ice by adding SDS-PAGE sample buffer (50 mM Tris pH 6.8, 100 mM DTT, 2% SDS, 0.1% bromophenol blue, 10% glycerol), followed by heating for 10 min at 95 °C. Protein samples were separated on SDS-PAGE gels followed by transferring to PVDF membranes (Thermo Fisher Scientific). Membranes were blocked in 5% non-fat milk (Bio-Rad) in TBS containing 0.1 % Tween-20 (TBST) for 1 h, followed by incubation overnight with primary antibodies at 4 °C. After 3 × 10 min washes in TBST, membranes were incubated with anti-mouse IgG horseradish peroxidase (HRP)-conjugated secondary antibodies at room temperature for 1 h. Membranes were then washed 3 × 10 min in TBST at room temperature and visualized using chemiluminescence by exposing to ECL film (GE Healthcare).

To prepare tissue lysates, mouse tissues were dissected and snap-frozen in liquid nitrogen. Frozen tissues were thawed and homogenized on ice with homogenizer (U.S. Solid) in ice-cold RIPA buffer (150 mM NaCl, 50 mM Tris-HCl pH 8.0, 1% Triton X-100, 0.5% sodium deoxycholate, 0.1% SDS) with 1 × protease inhibitors (Roche). After centrifugation at 16,000 g for 20 min at 4 °C, supernatants were collected for immunoblotting as described above. Proteins in mouse tissue fractions collected from sucrose density gradients were precipitated by trichloroacetic acid (TCA) and resuspended in 2 × SDS-containing sample buffer. To detect HiBiT-tagged proteins by Nano-Glo HiBiT blotting system (Promega), cell lysates were resolved by SDS-PAGE and transferred to PVDF membranes as described above. The membrane was incubated with 1 × TBST for 1 h at room temperature, followed by incubation in the LgBiT/buffer solution (50 μl of LgBiT protein in 10 ml of Nano-Glo blotting buffer) at room temperature for 1 h. 20 μl of substrate was added to the incubation solution for additional 5 min. The membrane was exposed to ECL film in the same manner as the immunoblot analysis.

shRNA knockdown

shRNAs targeting Rps26 and ABCE1 were designed from BROAD RNAi consortium database and subcloned into DECIPHER pRSI9-U6- (sh)-UbiC-TagRFP-2A-Puro (Cellecta). A scrambled shRNA was used as control. Lentiviral particles were produced using Lenti-X 293T cells (Clontech). The supernatants containing viral particles were harvested at 48 h after transfection and filtered through a 0.45 μM Millex-HP filter unit (Millipore). HEK293 cells were transduced with shRNA lentivirus for 48 h followed by selection with 2 μg/ml puromycin. Knockdown efficiency was detected by immunoblotting using indicated antibodies. The oligonucleotide sequences are listed in the Key Resources Table.

Polysome profiling

A total of 4 plates (10-cm) HEK293 cells grown to 80% confluency were washed by cold PBS and lysed in the polysome lysis buffer (10 mM HEPES, pH 7.4, 100 mM KCl, 5 mM $MgCl_2$, 100 μg/mL cycloheximide with 1% Triton X-100). The nuclei were pelleted by spinning at 14,000 rpm for 10 min at 4 °C. For mouse tissues, 100 mg of frozen samples were homogenized on ice using a Dounce homogenizer in 1 mL polysome lysis buffer. Homogeneous lysates were cleared by centrifugation at 14,000 rpm for 10 min at 4 °C. 500 μL of lysates were loaded onto a 15-45% (wt/vol) sucrose density gradients freshly prepared in a SW41 ultracentrifuge tube (Backman) using a Gradient Master (BioComp Instruments). Samples were centrifuged at 180,000 g for 2 h 30 min at 4 °C in a Beckman SW41 rotor. Polysome profiles were recorded at A254 using the Brandel Gradient Fractionation System and an ISCO UA-6 UV/Vis detector.

Ribosome profiling

The Ezra-seq has been described previously [22]. In brief, an aliquot of ribosome fractions representing monosome or polysome were collected followed by digestion with *E. coli* RNase I (Ambion, 750 U per 100 A260 units) by incubation at 4 °C for 1 h. RNA was extracted using Trizol LS reagent (Invitrogen) followed by ethanol precipitation. The ribosome-protected mRNA fragments (RPFs) were separated on a 15% polyacrylamide TBE-urea gel (Invitrogen) and visualized using SYBR Gold (Invitrogen). Selected regions in the gel corresponding to 25-35 nt were excised and dissolved by soaking in 400 μl RNA elution buffer (300 mM NaOAc pH 5.2, 1 mM EDTA, 0.1 U/μl SUPERase·In) for 10 min at 70 °C. The gel debris was removed using a Spin-X column (Corning), followed by ethanol precipitation. 14 μl RNAs (10∼200 ng) were mixed with 1 μl T4 PNK (NEB), 20 U SUPERase·In in 1 × T4 PNK buffer and incubated at 37 °C for 30 min followed by 65 °C for 20 min. After ethanol precipitation, 10 μl dissolved RNA were mixed with 1 μl homemade Ezra enzyme, 1 μl Poly(A) Polymerase (NEB) and 20 U SUPERase·In in 7 μl Ezra buffer. After incubation at 37 °C for 30 min followed by 65 °C for 20 min, 1 μl of 1 μM 5' end adaptor, 1 μl of 1 μM biotinylated reverse transcription primer, 20 U SUPERase·In were added and incubated at 70 °C for 3 min followed by slowly cooling down (3 °C/min) to 25 °C. The hybridized RNA sample was mixed with 10 μl of pre-washed streptavidin beads and incubated at room temperature for 10 min. Beads were washed and re-suspended in 10 μl nuclease-free water. Ligation was performed for 60 min at 25 °C by mixing beads with a 10 μl reaction mixture (1 × T4 Rnl2 reaction buffer, 20 U SUPERase·In, 15% PEG8000 and 200 U T4 RNA ligase 2 truncated KQ (NEB)). After washing once with 2 × SSC, beads were re-suspended in 12 μl nuclease-free water and mixed with 8 μl cDNA synthesis mixture (5 × first strand buffer, 0.1 M DTT, 10 mM dNTP, RNaseOUT and SuperScript III) followed by incubation at 50 °C for 30 min. After washing once with 2 × SSC, beads were resuspended in 10 μl nuclease-free water and incubated at 95 °C for 2 min, then immediately placed on the ice for 1 min. After placing on magnet stand for 1 min, the supernatant cDNA was amplified by PCR using barcoded sequencing primers. PCR was performed by mixing 1 × HF buffer, 0.5 mM dNTP, 0.25 μM PCR primers and 0.025 U Phusion polymerase. PCR was carried out under the following conditions: 98 °C, 30 s; (98 °C, 5 s; 68 °C, 15 s; 72 °C, 10 s) for 12 cycles; 72 °C, 3 min. PCR products were separated on a 8% polyacrylamide TBE gel (Invitrogen). DNA products with the expected size 180 bp were excised and recovered from DNA elution buffer (300 mM NaCl, 1 mM EDTA). After

quantification by Agilent BioAnalyzer DNA 1000 assay, equal amounts of barcoded samples were pooled and sequenced using NextSeq 500 (Illumina). The oligonucleotide sequences are listed in the Key Resources Table.

eRF1-seq

A total of 4 plates (10-cm) HEK293 cells with 80% confluence were washed three times with ice-cold DPBS. Cells were fixed in ice-cold formaldehyde solution (0.5% in DPBS) for 10 min at 4 °C on a rocker. After washing with ice-cold DPBS three times, cells were quenched in ice-cold buffer (50 mM Glycine, 50 mM Tris-HCl pH 7.5 in nuclease-free water) for 10 min at 4 °C on a rocker. Cells were then washed with polysome buffer and lysed in the 400 µl of polysome lysis buffer with 1% Triton-X-100 on ice. Cell debris was removed by centrifugation at 15,000 rpm for 10 min at 4 °C. The supernatant was digested with RNase I (Ambion, 750 U per 100 A260 units) for 1 h at 4 °C. Digested supernatant was loaded onto sucrose gradients for polysome profiling as described above. The 80S fraction was collected (~200 µl total) and mixed with 10 µg eRF1 antibody and 0.5 U/µl SUPERase·In (Invitrogen) followed by incubation under gentle rotation at 4 °C for 5 h. Protein A/G beads were added into the mixture and rotated at 4 °C overnight. Beads were washed three times and then resuspended in 600 µl of polysome buffer. RNA was extracted from resuspended beads in polysome buffer. Briefly, samples were brought to room temperature and then adjusted to 10 mM Tris-HCl pH 7.4, 10 mM glycine, 1% (w/v) SDS and 10 mM EDTA pH 8.0 followed by incubation at 65 °C for 5 min. One volume of acidic phenol/chloroform solution was added and vortexed at maximum speed for 2 min. Mixtures were then placed into thermomixer and shake at 1,400 rpm for 20 min at 65 °C to reverse the cross-links. After centrifugation at 14,000 rpm for 5 min at 4 °C, the aqueous phase was precipitated with ethanol. Purified RNA was used for cDNA library construction and high-throughput sequencing as described above.

Massively paralleled reporter assay (MPRA)

From the PCR product of HiBiT-EGFP described above, a second PCR was conducted using the pooled oligonucleotide library (IDT) and a primer containing the T7 promoter. The DNA template (1~2 µg) was utilized to generate the mRNA library via in vitro transcription as described above. Cells with 80% confluence were transfected with 6 µg of mRNA library using Lipofectamine MessengerMAX. Cells were lysed 4 h after transfection followed by polysome profiling as described above. Fractions of 500 µl corresponding to monosome or polysome were collected for RNA extraction using TRIzol LS. RNA was purified using RNA Clean & Concentrator and eluted with 11 µl of nuclease-free water. The purified RNA was reverse transcribed using SuperScript III and gene-specific primers. In brief, RNA samples were mixed with 1 µl of 10 mM dNTP, 2 pmol reverse primer and incubated at 65 °C for 5 min, then immediately placed on ice for 1 min. The reverse transcription was carried out by incubating with the 7 µl reaction mixture (5 × first strand buffer, 0.1 M DTT, RNaseOUT and SuperScript III) at 50 °C for 60 min followed by heating at 70 °C for 15 minutes. The products were then amplified with Illumina-based sequencing primers with barcode. PCR were performed by mixing 1 × HF buffer, 0.5 mM dNTP, 0.25 µM PCR primers and 0.025 U Phusion polymerase. The PCR was initiated at 98 °C, 30 s; then (98 °C, 5 s; 68 °C, 15 s; 72 °C, 10 s) for 12 cycles; 72 °C, 3 min. The PCR products with the expected size 190 bp were excised from a 8% polyacrylamide TBE gel. The DNA products were recovered from DNA elution buffer, followed by quantification using Agilent BioAnalyzer DNA 1000 assay. Equal amounts of barcoded samples were pooled for sequencing using NextSeq 500 (Illumina). The oligonucleotide sequences are listed in the Key Resources Table.

Structural analysis

To gain insights about the relative orientations and interaction likelihood between the 5' end of the mRNA (site -13 to -3 related to the A-site) and the 3' end of the 18S rRNA along the ribosome translocation, a structural analysis was carried using the respective PDBs 6GZ3 (with a 3.60 Å resolution), 6GZ4 (3.60 Å), 6GZ5 (3.50 Å) and 6yal (3.00 Å). The PDBs 6GZ3, 6GZ4 and 6GZ5 encompass three respective intermediate snapshots between the PRE and the POST translocation steps for the eukaryotic 80S ribosome (hereafter, referred simply as PRE and POST states). These three structures (hereafter referred as translocation intermediates POST 1 to 3, or simply TI-POST

1 – 3 for the respective PDBs 6GZ3 – 5) were solved, described and discussed previously [33]. The mRNA environment sequentially described by these three PDBs provides a reasonable glimpse about the changes occurring after the recognition of at the A site codon and along the movement of the ribosome to the next codon. The PDB 6YAL, in turn, is the Homo sapiens 48S late-stage initiation complex [53]. Due to the higher resolution of the PDB 6YAL, its mRNA structure is solved until a higher 5' extension compared to the 6GZ3–5 PDBs (The mRNA 5' in 6YAL starts from the -18 nt related to the site A, while in 6GZ3 it starts from the site -7 and from the site -6 in 6GZ4 and 6GZ5). In this way, we have made use of the 5' fragment of the 6YAL mRNA structure to build a rigid body model of the same extension starting from the -13 nt at each one of the PDBs 6GZ3–5, using structural alignment of the respective backbone atoms in each oligonucleotide extremity in Pymol [Schrodinger, LLC. 2010. The PyMOL Molecular Graphics System, Version 2.5].

Anisotropic network modeling

The relative local fluctuations of the exit mRNA channel at the ribosome structure and the consequent proximity likelihood between the mRNA 5' extension and the rRNA 3' end was estimated in presence and absence of Rps26 by normal mode analysis (NMA) using anisotropic network modeling (ANM) [54]. For this analysis, we used the atoms from the PDB 6YAL around a 30 Å region centered on Rps26 (depicting the mRNA channel exit) both in the presence and absence of this protein. The PDB 6YAL was chosen due to its higher resolution as a whole, besides longer extension of the mRNA 5' end compared to the other three PDBs structurally analyzed in this study. Furthermore, the region around 30 Å from Rps26 (hereafter called Rps26 site) encompass a symmetric sphere composed basically of residues from the 40S subunit (including the 18S 3' extension), mRNA (sites -13 to +5 nt related to the A-site) and the anti-codon loop from the P-site tRNA, common to all the four structures here analyzed. Finally, this region in 6YAL presents a relatively small global root mean square deviation (RMSD), considering the protein and RNA backbone, related to both PDBs 6GZ3 and 6GZ5 (1.478 Å in the two cases). In this way, the PDB 6YAL was considered an accurate approximation of the general environment of the Rps26/mRNA 5' end/rRNA 3' end triad in ribosome, despite portraying a pre-initiation structure.

The ANM was carried using the ProDy tools [55–57]. A Hessian matrix was built upon the backbone atoms of the Rps26 site for both proteins (Cα) and RNA (P, C4' and C2) with and without Rps26 (hereafter referred as + Rps26 and – Rps26). The mRNA was considered from the -10 to the +5 nt, once the first three residues (-13 to -11) are more distant from the rRNA 3' end and free of direct contacts with the neighborhood as a whole, which makes their movements dominate the NMA if they are considered on the ANM (not shown). The Hessian matrix was configured using the default parameters of distance cutoff and gamma function, with the respective values of 15 Å and 1.0 kcal/(mol.Å2). Initially, the first 50 normal modes of each system were estimated by obtaining their respective covariance matrixes by diagonalizing the Hessiam matrixes. The modes simultaneously containing the largest possible eigenvalues and higher mRNA fluctuations at the -10 to -3 extension (directly parallel to the rRNA 3' end and separated from it by Rps26), as well as the fluctuations of the last 10 residues at the 18S 3' end, were selected. In this way, the 15 first ANM normal modes estimated from the + Rps26 and – Rps26 systems were taken for conformational sampling analysis.

The +Rps26 and –Rps26 structures of the Rps26 site from above were taken to sampling of alternate conformations along the global fluctuations described by their respective 15 first ANM modes using ProDy [55–57]. Basically, an extended ANM model containing all the protein and rRNA atoms for each structure was built from the original coarse grain model containing only the backbone atoms used to build the Hessian matrix. All the atoms at the extended model still obey the movements dictated by the selected 15 first normal modes, with each side chain atom moving in the same direction that the backbone atoms of the residue to which they belong. A set of 70 conformations symmetrically distributed along the fluctuation governed by the 15 first normal modes and with an average RMSD of 2.5 Å related to the input structure was sampled for each one of the +Rps26 and –Rps26 models. Finally, from each original 70 conformers set, a subset containing only the sterically feasible structures (i.e., without significant clashes or conformational distortions) was taken for analysis. Although higher refinements would be

necessary to take these final conformers to rigorous molecular dynamics or free energy calculation studies, they provide enough insights about the Rps26 influence on the mRNA 5' end/18S 3' end fluctuations and interaction distance likelihood at the ribosome context.

Quantification and statistical analysis

Data is presented as mean ± SEM, unless otherwise stated. At least three independent biological replicates have been performed for each experiment. The number of independent experiments is indicated. Statistical tests used and specific p-values are indicated in the figure legends.

Analysis of Ribo-seq and eRF1-seq

The adaptor of sequencing reads was clipped by Cutadapt, using parameters: -a AAAAAA --max-n=0.1 -m 15. The clean reads were then aligned to human transcriptome (GRCh38.81), which contains the protein coding transcripts with the longest CDS, using STAR with default parameters. To avoid ambiguity, reads mapped to multiple positions or with > 2 mismatches were disregarded for further analysis. Ribosome P-site was defined as the positions of 12th, 13th and 14th from 5' end of the read (position 0). A-site was defined as the positions of 15th, 16th and 17th. To generate aggregation plot around the start and stop codons, for each mRNA, the aligned reads at individual sites were normalized by mean reads of the CDS. mRNAs with total reads in CDS < 16 or the CDS sites covered by footprints < 10% were excluded. The normalized values of the sites with the same distance relative to the start codon or stop codon were averaged across transcriptome.

Identification of termination peaks

To identify termination peaks, all reads of eRF1-seq were assigned to individual sites on mRNAs. The mRNAs with < 10 total reads from eRF1-seq were excluded. A 120-nt sliding window was used to scan along the mRNA, the sites with terminating reads tenfold higher than the average reads within the sliding window were defined as the termination peaks.

uORF prediction

For each mRNA, all possible uORFs starting with AUG were first extracted. A Wilcoxon test was applied to test whether the in-frame reads are significantly higher than the other two frames. The two *P* values were then combined to a single *P* value using a Stouffer's method. uORFs with a false discovery rate (FDR) <0.05 were defined as the uORFs with robust translation.

RNA secondary structure analysis

A 30-nt sliding window was used to scan 3' UTR. For each window, the minimum fold free energy (MFE) was calculated by ViennaRNA [PMID: 22115189] using default parameters.

Analysis of MPRA dataset

For each raw sequencing file, the adaptors at both ends were removed by cutadapt. The trimmed reads with length unequal to 9 nucleotides were excluded from analysis. The remaining trimmed reads were counted and then an RPM value (reads per million) was obtained by dividing the resultant read count by the total count.

Data availability

All Sequencing data are available in the Gene Expression Omnibus database.

Acknowledgements

We thank Cornell University Life Sciences Core Laboratory Center for sequencing and FACS. S.U. was supported by Takeda Science Foundation. This work was supported by US National Institutes of Health (DP1GM142101) and HHMI Faculty Scholar (55108556) to S.-B.Q.

Additional information

Author contributions

S.-B.Q. conceived the project. L.J. performed most experiments. Y.M. conducted the majority of sequencing data analysis. S.U. performed data analysis involving 18S rRNA and Rps26. A.X.L. performed tissue polysome analysis of Rps26. L.D. contributed to the sequencing of mouse tissues. L.H.F.L. conducted ribosome structural analysis. S.-B.Q. wrote the manuscript. All authors initially discussed the results and edited the manuscript.

Funding

Funder	Grant reference number	Author
NIH Office of the Director (OD)	DP1GM142101	Shu-Bing Qian
Howard Hughes Medical Institute (HHMI)	55108556	Shu-Bing Qian

Author ORCID iDs

Shu-Bing Qian: https://orcid.org/0000-0002-4127-1136

Additional files

Supplementary Fig 1 - 7

References

1. **Hellen C.U.T** (2018) Translation Termination and Ribosome Recycling in Eukaryotes. *Cold Spring Harb Perspect Biol* **10** https://doi.org/10.1101/cshperspect.a032656 | PubMed
2. **Schuller A.P.,** Green R (2018) Roadblocks and resolutions in eukaryotic translation. *Nat Rev Mol Cell Biol* **19**:526-541 https://doi.org/10.1038/s41580-018-0011-4 | PubMed
3. **Pisarev A.V.,** Skabkin M.A., Pisareva V.P., Skabkina O.V., Rakotondrafara A.M., Hentze M.W., Hellen C.U., Pestova T.V (2010) The role of ABCE1 in eukaryotic posttermination ribosomal recycling. *Mol Cell* **37**:196-210 https://doi.org/10.1016/j.molcel.2009.12.034 | PubMed
4. **Young D.J.,** Guydosh N.R., Zhang F., Hinnebusch A.G., Green R (2015) Rli1/ABCE1 Recycles Terminating Ribosomes and Controls Translation Reinitiation in 3'UTRs In Vivo. *Cell* **162**:872-884 https://doi.org/10.1016/j.cell.2015.07.041 | PubMed
5. **Seoighe C.,** Kiniry S.J., Peters A., Baranov P.V., Yang H (2020) Selection Shapes Synonymous Stop Codon Use in Mammals. *J Mol Evol* **88**:549-561 https://doi.org/10.1007/s00239-020-09957-x | PubMed
6. **Palma M.,** Lejeune F (2021) Deciphering the molecular mechanism of stop codon readthrough. *Biol Rev Camb Philos Soc* **96**:310-329 https://doi.org/10.1111/brv.12657 | PubMed
7. **Wangen J.R.,** Green R (2020) Stop codon context influences genome-wide stimulation of termination codon readthrough by aminoglycosides. *eLife* **9** https://doi.org/10.7554/eLife.52611 | PubMed
8. **Mangkalaphiban K.,** He F., Ganesan R., Wu C., Baker R., Jacobson A (2021) Transcriptome-wide investigation of stop codon readthrough in Saccharomyces cerevisiae. *PLoS Genet* **17**:e1009538 https://doi.org/10.1371/journal.pgen.1009538 | PubMed
9. **Brown A.,** Shao S., Murray J., Hegde R.S., Ramakrishnan V (2015) Structural basis for stop codon recognition in eukaryotes. *Nature* **524**:493-496 https://doi.org/10.1038/nature14896 | PubMed
10. **Hudson A.M.,** Szabo N.L., Loughran G., Wills N.M., Atkins J.F., Cooley L (2021) Tissue-specific dynamic codon redefinition in Drosophila. *Proc Natl Acad Sci U S A* **118** https://doi.org/10.1073/pnas.2012793118 | PubMed
11. **Matsufuji S.,** Matsufuji T., Miyazaki Y., Murakami Y., Atkins J.F., Gesteland R.F., Hayashi S (1995) Autoregulatory frameshifting in decoding mammalian ornithine decarboxylase antizyme. *Cell* **80**:51-60 https://doi.org/10.1016/0092-8674(95)90450-6 | PubMed

12. **Annibaldis G.,** Domanski M., Dreos R., Contu L., Carl S., Klay N., Muhlemann O (2020) Readthrough of stop codons under limiting ABCE1 concentration involves frameshifting and inhibits nonsense-mediated mRNA decay. *Nucleic Acids Res* **48**:10259-10279 https://doi.org/10.1093/nar/gkaa758 | PubMed

13. **Skabkin M.A.,** Skabkina O.V., Hellen C.U., Pestova T.V (2013) Reinitiation and other unconventional posttermination events during eukaryotic translation. *Mol Cell* **51**:249-264 https://doi.org/10.1016/j.molcel.2013.05.026 | PubMed

14. **Ingolia N.T.,** Lareau L.F., Weissman J.S (2011) Ribosome profiling of mouse embryonic stem cells reveals the complexity and dynamics of mammalian proteomes. *Cell* **147**:789-802 https://doi.org/10.1016/j.cell.2011.10.002 | PubMed

15. **Dunn J.G.,** Foo C.K., Belletier N.G., Gavis E.R., Weissman J.S (2013) Ribosome profiling reveals pervasive and regulated stop codon readthrough in Drosophila melanogaster. *eLife* **2**:e01179 https://doi.org/10.7554/eLife.01179 | PubMed

16. **Sapkota D.,** Lake A.M., Yang W., Yang C., Wesseling H., Guise A., Uncu C., Dalal J.S., Kraft A.W., Lee J.M., *et al.* (2019) Cell-Type-Specific Profiling of Alternative Translation Identifies Regulated Protein Isoform Variation in the Mouse Brain. *Cell Rep* **26**:594-607.e597. https://doi.org/10.1016/j.celrep.2018.12.077 | PubMed

17. **Karki P.,** Carney T.D., Maracci C., Yatsenko A.S., Shcherbata H.R., Rodnina M.V (2022) Tissue-specific regulation of translational readthrough tunes functions of the traffic jam transcription factor. *Nucleic Acids Res* **50**:6001-6019 https://doi.org/10.1093/nar/gkab1189 | PubMed

18. **Amrani N.,** Ganesan R., Kervestin S., Mangus D.A., Ghosh S., Jacobson A (2004) A faux 3'-UTR promotes aberrant termination and triggers nonsense-mediated mRNA decay. *Nature* **432**:112-118 https://doi.org/10.1038/nature03060 | PubMed

19. **Karousis E.D.,** Gurzeler L.A., Annibaldis G., Dreos R., Muhlemann O (2020) Human NMD ensues independently of stable ribosome stalling. *Nat Commun* **11**:4134 https://doi.org/10.1038/s41467-020-17974-z | PubMed

20. **Keeling K.M.,** Xue X., Gunn G., Bedwell D.M (2014) Therapeutics based on stop codon readthrough. *Annu Rev Genomics Hum Genet* **15**:371-394 https://doi.org/10.1146/annurev-genom-091212-153527 | PubMed

21. **Ingolia N.T** (2014) Ribosome profiling: new views of translation, from single codons to genome scale. *Nat Rev Genet* https://doi.org/10.1038/nrg3645 | PubMed

22. **Mao Y.,** Jia L., Dong L., Shu X.E., Qian S.B (2023) Start codon-associated ribosomal frameshifting mediates nutrient stress adaptation. *Nat Struct Mol Biol* **30**:1816-1825 https://doi.org/10.1038/s41594-023-01119-z | PubMed

23. **Pisarev A.V.,** Hellen C.U., Pestova T.V (2007) Recycling of eukaryotic posttermination ribosomal complexes. *Cell* **131**:286-299 https://doi.org/10.1016/j.cell.2007.08.041 | PubMed

24. **Lawson M.R.,** Lessen L.N., Wang J., Prabhakar A., Corsepius N.C., Green R., Puglisi J.D (2021) Mechanisms that ensure speed and fidelity in eukaryotic translation termination. *Science* **373**:876-882 https://doi.org/10.1126/science.abi7801 | PubMed

25. **Shen L.,** Su Z., Yang K., Wu C., Becker T., Bell-Pedersen D., Zhang J., Sachs M.S (2021) Structure of the translating Neurospora ribosome arrested by cycloheximide. *Proc Natl Acad Sci U S A* **118** https://doi.org/10.1073/pnas.2111862118 | PubMed

26. **Orr M.W.,** Mao Y., Storz G., Qian S.B (2020) Alternative ORFs and small ORFs: shedding light on the dark proteome. *Nucleic Acids Res* **48**:1029-1042 https://doi.org/10.1093/nar/gkz734 | PubMed

27. **Gould P.S.,** Dyer N.P., Croft W., Ott S., Easton A.J (2014) Cellular mRNAs access second ORFs using a novel amino acid sequence-dependent coupled translation termination-reinitiation mechanism. *RNA* **20**:373-381 https://doi.org/10.1261/rna.041574.113 | PubMed

28. **Jia L.,** Mao Y., Ji Q., Dersh D., Yewdell J.W., Qian S.B (2020) Decoding mRNA translatability and stability from the 5' UTR. *Nat Struct Mol Biol* **27**:814-821 https://doi.org/10.1038/s41594-020-0465-x | PubMed

29. **Kesner J.S.,** Chen Z., Shi P., Aparicio A.O., Murphy M.R., Guo Y., Trehan A., Lipponen J.E., Recinos Y., Myeku N., *et al.* (2023) Noncoding translation mitigation. *Nature* **617**:395-402 https://doi.org/10.1038/s41586-023-05946-4 | PubMed

30. **Muller M.B.D.,** Kasturi P., Jayaraj G.G., Hartl F.U (2023) Mechanisms of readthrough mitigation reveal principles of GCN1-mediated translational quality control. *Cell* **186**:3227-3244.e3220. https://doi.org/10.1016/j.cell.2023.05.035 | PubMed

31. **Pisarev A.V.,** Kolupaeva V.G., Yusupov M.M., Hellen C.U., Pestova T.V (2008) Ribosomal position and contacts of mRNA in eukaryotic translation initiation complexes. *EMBO J* **27**:1609-1621 https://doi.org/10.1038/emboj.2008.90 | PubMed

32. **Brito Querido J.,** Sokabe M., Kraatz S., Gordiyenko Y., Skehel J.M., Fraser C.S., Ramakrishnan V. (2020) Structure of a human 48S translational initiation complex. *Science* **369**:1220-1227 https://doi.org/10.1126/science.aba4904 | PubMed

33. **Flis J.,** Holm M., Rundlet E.J., Loerke J., Hilal T., Dabrowski M., Burger J., Mielke T., Blanchard S.C., Spahn C.M.T., *et al.* (2018) tRNA Translocation by the Eukaryotic 80S Ribosome and the Impact of GTP Hydrolysis. *Cell Rep* **25**:2676-2688.e2677. https://doi.org/10.1016/j.celrep.2018.11.040 | PubMed

34. **Burman L.G.,** Mauro V.P (2012) Analysis of rRNA processing and translation in mammalian cells using a synthetic 18S rRNA expression system. *Nucleic Acids Res* **40**:8085-8098 https://doi.org/10.1093/nar/gks530 | PubMed

35. **Wan J.,** Gao X., Mao Y., Zhang X., Qian S.B (2018) A Coding Sequence-Embedded Principle Governs Translational Reading Frame Fidelity. *Research (Wash D C)* **2018**:7089174 https://doi.org/10.1155/2018/7089174 | PubMed

36. **Gobet C.,** Weger B.D., Marquis J., Martin E., Neelagandan N., Gachon F., Naef F (2020) Robust landscapes of ribosome dwell times and aminoacyl-tRNAs in response to nutrient stress in liver. *Proc Natl Acad Sci U S A* **117**:9630-9641 https://doi.org/10.1073/pnas.1918145117 | PubMed

37. **Sharifulin D.,** Khairulina Y., Ivanov A., Meschaninova M, SVen'yaminova A., SGraifer D., SKarpova G. (2012) A central fragment of ribosomal protein S26 containing the eukaryote-specific motif YxxPKxYxK is a key component of the ribosomal binding site of mRNA region 5' of the E site codon. *Nucleic Acids Res* **40**:3056-3065 https://doi.org/10.1093/nar/gkr1212 | PubMed

38. **Yang Y.M.,** Karbstein K (2022) The chaperone Tsr2 regulates Rps26 release and reincorporation from mature ribosomes to enable a reversible, ribosome-mediated response to stress. *Sci Adv* **8**:eabl4386 https://doi.org/10.1126/sciadv.abl4386 | PubMed

39. **Uhlen M.,** Fagerberg L., Hallstrom B.M., Lindskog C., Oksvold P., Mardinoglu A., Sivertsson A., Kampf C., Sjostedt E., Asplund A., *et al.* (2015) Proteomics. Tissue-based map of the human proteome. *Science* **347**:1260419 https://doi.org/10.1126/science.1260419 | PubMed

40. **Plassart L.,** Shayan R., Montellese C., Rinaldi D., Larburu N., Pichereaux C., Froment C., Lebaron S., O'Donohue M.F., Kutay U., *et al.* (2021) The final step of 40S ribosomal subunit maturation is controlled by a dual key lock. *eLife* **10** https://doi.org/10.7554/eLife.61254 | PubMed

41. **Shine J.,** Dalgarno L (1974) The 3'-terminal sequence of Escherichia coli 16S ribosomal RNA: complementarity to nonsense triplets and ribosome binding sites. *Proc Natl Acad Sci U S A* **71**:1342-1346 https://doi.org/10.1073/pnas.71.4.1342 | PubMed

42. **Tranque P.,** Hu M.C., Edelman G.M., Mauro V.P (1998) rRNA complementarity within mRNAs: a possible basis for mRNA-ribosome interactions and translational control. *Proc Natl Acad Sci U S A* **95**:12238-12243 https://doi.org/10.1073/pnas.95.21.12238 | PubMed

43. **Martin F.,** Menetret J.F., Simonetti A., Myasnikov A.G., Vicens Q., Prongidi-Fix L., Natchiar S.K., Klaholz B.P., Eriani G (2016) Ribosomal 18S rRNA base pairs with mRNA during eukaryotic translation initiation. *Nat Commun* **7**:12622 https://doi.org/10.1038/ncomms12622 | PubMed

44. **Yueh A.,** Schneider R.J (2000) Translation by ribosome shunting on adenovirus and hsp70 mRNAs facilitated by complementarity to 18S rRNA. *Genes Dev* **14**:414-421 https://doi.org/10.1101/gad.14.4.414 | PubMed

45. **Varani G.,** McClain W.H (2000) The G x U wobble base pair. A fundamental building block of RNA structure crucial to RNA function in diverse biological systems. *EMBO Rep* **1**:18-23 https://doi.org/10.1093/embo-reports/kvd001 | PubMed

46. **Soumillon M.,** Necsulea A., Weier M., Brawand D., Zhang X., Gu H., Barthes P., Kokkinaki M., Nef S., Gnirke A., *et al.* (2013) Cellular source and mechanisms of high transcriptome complexity in the mammalian testis. *Cell Rep* **3**:2179-2190 https://doi.org/10.1016/j.celrep.2013.05.031 | PubMed

47. **Jones S.H.,** Wilkinson M (2017) RNA decay, evolution, and the testis. *RNA Biol* **14**:146-155 https://doi.org/10.1080/15476286.2016.1265199 | PubMed

48. **Allen S.R.,** Stewart R.K., Rogers M., Ruiz I.J., Cohen E., Laederach A., Counter C.M., Sawyer J.K., Fox D.T (2022) Distinct responses to rare codons in select Drosophila tissues. *eLife* **11** https://doi.org/10.7554/eLife.76893 | PubMed

49. **Sun Y.H.,** Li X.Z (2019) Ribosomes mediate pachetene piRNA formation on long intergenic piRNA precursors. *Nat Cell Biol* https://doi.org/10.1038/s41556-019-0457-4 | PubMed

50. **Ferretti M.B.,** Ghalei H., Ward E.A., Potts E.L., Karbstein K (2017) Rps26 directs mRNA-specific translation by recognition of Kozak sequence elements. *Nat Struct Mol Biol* **24**:700-707 https://doi.org/10.1038/nsmb.3442 | PubMed

51. **Boria I.,** Garelli E., Gazda H.T., Aspesi A., Quarello P., Pavesi E., Ferrante D., Meerpohl J.J., Kartal M., Da Costa L., *et al.* (2010) The ribosomal basis of Diamond-Blackfan Anemia: mutation and database update. *Hum Mutat* **31**:1269-1279 https://doi.org/10.1002/humu.21383 | PubMed

52. **Mills E.W.,** Wangen J., Green R., Ingolia N.T (2016) Dynamic Regulation of a Ribosome Rescue Pathway in Erythroid Cells and Platelets. *Cell Rep* **17**:1-10 https://doi.org/10.1016/j.celrep.2016.08.088 | PubMed

53. **Simonetti A.,** Guca E., Bochler A., Kuhn L., Hashem Y (2020) Structural Insights into the Mammalian Late-Stage Initiation Complexes. *Cell Rep* **31**:107497 https://doi.org/10.1016/j.celrep.2020.03.061 | PubMed

54. **Atilgan A.R.,** Durell S.R., Jernigan R.L., Demirel M.C., Keskin O., Bahar I (2001) Anisotropy of fluctuation dynamics of proteins with an elastic network model. *Biophys J* **80**:505-515 https://doi.org/10.1016/S0006-3495(01)76033-X | PubMed

55. **Zhang S.,** Krieger J.M., Zhang Y., Kaya C., Kaynak B., Mikulska-Ruminska K., Doruker P., Li H., Bahar I (2021) ProDy 2.0: increased scale and scope after 10 years of protein dynamics modelling with Python. *Bioinformatics* **37**:3657-3659 https://doi.org/10.1093/bioinformatics/btab187 | PubMed

56. **Bakan A.,** Meireles L.M., Bahar I (2011) ProDy: protein dynamics inferred from theory and experiments. *Bioinformatics* **27**:1575-1577 https://doi.org/10.1093/bioinformatics/btr168 | PubMed

57. **Bakan A.,** Dutta A., Mao W., Liu Y., Chennubhotla C., Lezon T.R., Bahar I (2014) Evol and ProDy for bridging protein sequence evolution and structural dynamics. *Bioinformatics* **30**:2681-2683 https://doi.org/10.1093/bioinformatics/btu336 | PubMed

Peer reviews

Reviewer #2 (Public review):

Summary:

This paper presents results interpreted to indicate that sequences upstream of stop codons capable of base-pairing with the 3' end of 18S rRNA prolong the dwell time of 80S ribosomes at stop codons in a manner impeded by Rps26 in the 40S subunit exit channel, which leads to the proper completion of termination and ribosome recycling and prevents spurious translation of 3'UTR sequences by one or more unconventional mechanisms.

Strengths:

The standard 80S and selective eRF1 80S ribosome profiling data obtained using EZRA-Seq are of high quality, allowing the authors to detect an enrichment for purine-rich sequences upstream of stop codons at sites where termination is relatively slow and ribosomal complexes are paused with eRF1 still engaged in the A site.

Weaknesses:

There are many weaknesses in the experimental design and interpretation of results that undermine several of the final conclusions of the study described in the abstract, as described in detail below.

(1) It's not indicated how far upstream of the stop codon the sequences were searched to find the enriched motifs in Figs. 1C and 2D. If it's further upstream of -15 then the sequence would generally not be found in the exit channel of a terminating ribosome positioned with the stop codon in the A site in the manner expected from their final model of mRNA:18S rRNA pairing. (This would be analogous to the occurrence of the Shine-Dalgarno within 15 nt of the initiation codon for most mRNAs in E. coli.) They could have depicted nucleotide percentages at each nucleotide from -1 to -15 for the high and low pause stop codons to better facilitate consideration of their proposed mechanism of termination pausing involving the 3' end of 18S rRNA.

(2) lines 234-242: Their reporter data in Fig. 4B suggest that only the presence of GGG triplets at any location in the 9 nt substantially prevents downstream translation. If their interpretation about these G-rich sequences promoting termination by forming G-quadruplexes is correct, then this would have little to do with the purine-rich motifs identified by the profiling experiments (and their proposed function in base-pairing with rRNA), as the purine-rich motifs do not feature GG bases (as shown in Fig. 2D in particular). The authors point out that the MPRA can sample sequence space not represented in living cells. While true, this doesn't change the fact that it failed identify sequences conforming to the purine rich motifs found by the profiling experiments and identified instead sequences capable of forming G-quadruplexes that may well function by a different mechanism than that employed in cells. The authors cannot persist in claiming that the MPRA results confirm the findings of the profiling experiments regarding the purine-rich motif. Also, the claim of enrichment for C-rich sequences in the MPRA results is not compelling as only 3 of the 11 triplets showing the smallest M/P ratios contain more than 1 C and three of them contain no Cs. Also, there was no evidence for depletion of C's upstream of the stop codons with low pause scores from the ribosome profiling data in Fig. 1, so it's inaccurate to claim "mirroring" of results from the ribosome profiling and MPRA data on this point as well.

(3) lines 256-260: I still contend that the different results shown in Fig. 4E for the C-rich and GA-rich sequences are not compelling as results for only a single sequence of each type are shown, which might not be typical of the entire class. In fact, the GA-rich sequence has two GG's and could form a G-quadruplex, whereas the GA-rich motifs identified by ribosome profiling and eRF1-seq do not exhibit consecutive GGs, such that the single G-rich sequence chosen for analysis might function by G-quadruplex mediated stalling rather than base-pairing with the 3' end of 18S rRNA, as they actually suggested in their rebuttal. Even the second GA-rich sequence analyzed in Fig. S3G has two GGs. Thus, while the results in Fig. 4 provide support for the notion that C-rich sequences preceding the stop codon promote stop codon read-through, it's important to note that no evidence was obtained by ribosome-profiling in Fig. 1 that the increased 3'UTR translation seen for low-pause stop codons is associated with C-rich sequences. It's unclear why they would be unable to observe this in the manner they document for the eRF1-Seq data in Fig. 2D for the three C-rich triplets enriched at stop codons lacking eRF1 peaks.

- lines 278-282: These differences are quite small and could arise from the different sequences of the GFP-HiBit fusion proteins, as observed in Fig. 4C (top two control constructs),

precluding mechanistic interpretations.

(4) Notwithstanding their claim in the rebuttal, I still find no definition of the GA-rich and C-rich mRNAs described in Fig. 5C in the Methods or legends, nor whether the compilation is restricted to -15 from the stop codons. In addition, if expression of the mutant 18S rRNA is sufficient to alter the height of the termination peaks as shown in Fig. 5C and to alter reporter expression in Fig. 5D, I see no reason why they cannot carry out the pause score/motif enrichment of Fig. 1C to determine if they see the expected diminished enrichment for the GA-motif shown there on expressing the mutant 18S vs. the WT 18S control strain. If not, this would undermine their interpretation of the results in Figs. 5C-D as favoring base-pairing between the 3' end of 18S rRNA and sequences upstream of the stop codon.

(5) I still find a significant shortcoming in their failure to analyze the 18S rRNA 3' end biochemically to show that the expected ~15% with the mutant sequence. Stating simply that they followed a previous protocol is not sufficient to document their success in this notoriously challenging experimental approach.

(6) lines 382-384: The level of the control protein RACK1 is diminished in testis polysomes, and it's unclear that the ratio of Rps26:RACK1 is actually lower in testis polysomes in the manner claimed.

(7) lines 414-427: I still contend that the authors should have quantified the ratio of the stop codon peak to the adjacent coding sequences in Figures 7E to establish that Rps26 OE decreased the stop codon peaks selectively on the GA-rich cohort of mRNAs. In addition, they still have not explained why the C-rich reporter behaves like the GA-rich reporter in Fig. 7F in showing reduced HiBiT expression on Rps26 OE when it should be unaffected. As such, the reporter data do not support the conclusion reached from the data in Fig. 7E.

(8) Notwithstanding their rebuttal I still contend that the failure to measure Rps26 association with 80S ribsoomes or polysomes and show that it is depleted by the shRNA knockdown and increased by Rps26 OE is a significant shortcoming, especially since their interpretation of the OE data depends on the occurrence of 40S subunits lacking Rps26 in unstressed WT cells, which seems improbable based on the prior work on yeast.

(9) Overall, examining the claims in the revised Abstract, I feel that I am in agreement with the claim "We identify a sequence motif upstream of the stop codon that promotes termination pausing,.." but disagree that the function of this motif was "validated by massively paralleled reporter assays", for the reasons stated above in point 2. Regarding the statement "Unexpectedly, reduced termination pausing increases the likelihood of stop codon slippage, giving rise to proteins with heterogenous C-terminal extensions." , I believe it would be more cautious to say that "reduced pausing is associated with stop codon read-through accompanied by frameshifting" since the MRPA did not provide compelling evidence for causality for the reasons described in point 3 above. Regarding the statement "Mechanistically, we show that sequence-dependent termination pausing arises from post-decoding mRNA scanning by the 3' end of 18S rRNA", I find this statement too strong in view of the shortcomings described above in points 4-5 and think it would be more correct to say that their findings are consistent with (rather than showing) this point, and also think they should add qualifying statements to the manuscript acknowledging the limitations of these experiments. I further contend that there are shortcomings in the experiments leading to the conclusion that the stoichiometry of Rps26... modulates mRNA:rRNA interactions, described above in points 6-9. Finally, in the last sentence, the claims that termination pausing is shaped by ribosome heterogeneity, and cell type-specific translational control is too strong.

https://doi.org/10.7554/eLife.109257.2.sa2

Reviewer #3 (Public review):

Summary:

This study from Jia et al carried out a variety of analyses of terminating ribosomes, including the development of eRF1-seq to map termination sites, identification of a GA-rich motif that promotes ribosome pausing, characterization of tissue-specific termination dynamics, and elucidation of the regulatory roles of 18S rRNA and RPS26. Overall, the study is thoughtfully designed, and its biological conclusions are well supported by complementary experiments. The tools and datasets generated provide valuable resources for researchers investigating the mechanisms of RNA translation.

Strengths:

(1) The study introduces eRF1-seq, a novel approach for mapping translation termination sites, providing a methodological advance for studying ribosome termination.

(2) Through integrative bioinformatic analyses and complementary MPRA experiments, the authors demonstrate that GA-rich motifs promote ribosome pausing at termination sites and reveal possible regulatory roles of 18S rRNA in this process.

(3) The study characterizes tissue-specific ribosome termination dynamics, showing that the testis exhibits stronger ribosome pausing at stop codons compared to other tissues. Follow-up experiments suggest that RPS26 may contribute to this tissue specificity.

Weaknesses:

The biological significance of ribosome pausing regulation at translation termination sites or of translational readthrough, for example across different tissue types, remains unclear. Nevertheless, this question lies beyond the primary scope of the current study.

Comments on the latest version:

The authors addressed my comments by revising the claims in the manuscript.

https://doi.org/10.7554/eLife.109257.2.sa1

Author response:

The following is the authors' response to the original reviews.

We thank the Editor and Reviewers for their careful evaluation of our manuscript and for the constructive feedback. We agree with eLife's overall assessment that, while profiling terminating ribosomes provides important insights into termination dynamics, additional clarification of the underlying mechanisms was needed. In response, we have focused our revision on three major conceptual points:

(1) We have moderated our interpretation regarding the contribution of putative mRNA:rRNA interactions to sequence-specific termination pausing and clarified the limitations of the current evidence.

(2) We have refined and clarified our model for the role of Rps26 in regulating translation termination.

(3) We have expanded and strengthened the discussion of tissue-specific termination pausing, including its potential implications and current uncertainties.

> ***Public Reviews:***

> ***Reviewer #1 (Public review):***
>
> *Summary:*
>
> *The authors use high-resolution ribosome profiling (Ezra-seq) and eRF1 pulldown-based ribosome profiling (eRF1-seq) developed in their lab to identify a GA rich sequence motif located upstream of the stop codon responsible for translation termination pausing. They then perform a massively parallel assay with randomly generated sequences to further characterize this motif. Using mouse tissues, they show that termination pausing signatures can be tissue-specific. They use a series of published ribosome structures and 18S rRNA mutants, and eS26 knockdown experiments to propose that the GA rich sequence interacts with the 3'-end of the 18S rRNA.*
>
> *Strengths:*
>
> *(1) Robust ribosome profiling data and clear analyses clarify the subtle behavior of terminating ribosomes near the stop codon.*
>
> *(2) Novel termination or "false termination" sites revealed by eRF1-seq in the 5'-UTR, 3'-UTR, and CDS highlight a previously underappreciated facet of translation dynamics.*
>
> *Weakness:*
>
> *(1) Modest effects seen in ABCE1 knockdown do not seem to add up to the level of regulation. The authors state "ABCE1 regulates terminating ribosomes independent of the sequence context" on pg 9, and "ABCE1 modulates termination pausing independent of the mRNA sequence context" in the figure caption for Figure S4. Given the modest effect of the knockdown, such phrasing is most likely not supported. Further clarification of "ABCE1 plays a generic role in translation termination" is necessary.*

We acknowledge that the modest effects observed for ABCE1 are likely influenced by incomplete knockdown in HEK293 cells. Importantly, the increased ribosome density occurred at all stop codons rather than in a sequence-dependent manner, supporting the conclusion that ABCE1 functions broadly in termination rather than acting in a sequence-specific context. We have revised the manuscript to clarify this point and to temper our interpretation accordingly.

> *(2) The authors propose that the GA rich sequence element upstream of the stop codon on the mRNA could potentially base pair with the 3'-end of the 18S rRNA. In the PDBs the authors reference in their paper and also in 3JAG, 3JAH, 3JAI (structures of terminating ribosomes with the stop codon in the A-site and eRF1), the mRNA exiting the ribosome and the 3'-end of the 18S rRNA are about 25-30 A apart. In addition, a segment of eS26 is wedged in between these two RNA segments. This reviewer noted this arrangement in a random sampling of 5 other PDBs of mammalian and human ribosome 80S structures. How do the authors anticipate the base pairing they have proposed to occur in light of these steric hindrances? RpsS26 is known to be released by Tsr2 in yeast during very specific stresses. Is it their expectation that termination pausing in human/mammalian cells happens during stressful conditions only?*

We agree that structural rearrangements in the absence of Rps26 remain speculative. In the revised manuscript, we have removed overly definitive language and clarified that, while Rps26 dissociation has been reported under stress conditions, its stoichiometry is unlikely to be exclusively stress-dependent. We now present this aspect as a working model supported by indirect evidence rather than a demonstrated structural mechanism.

> *(3) The authors say, "It is thus likely that mRNA undergoes post-decoding scanning by 18S rRNA." (pg. 10). It is unclear what the authors mean by "scanning." Do they mean*

> *that the mRNA gets scanned in a manner similar to scanning during initiation? There is no evidence presented to support that particular conclusion.*

We appreciate the comment regarding the term "18S rRNA scanning." We recognize that this wording may have been misleading and have revised the relevant text to more accurately describe post-decoding mRNA–rRNA interactions without implying an active scanning mechanism.

> *(4) Role of termination pausing in the testis is highly speculative. The authors state: "It is thus conceivable that the wide range of ribosome density at stop codons in testis facilitates functional division of ribosome occupancy beyond the coding region." It is unclear what type of functional division they are referring to.*

We agree that the functional significance of testis-specific termination dynamics remains unclear. As multiple reviewers raised this concern, we have substantially expanded the discussion of tissue-specific termination pausing, explicitly outlining current limitations and framing this as an important direction for future investigation.

> ***Reviewer #2 (Public review):***
>
> *Summary:*
>
> *This paper presents results interpreted to indicate that sequences upstream of stop codons capable of base-pairing with the 3' end of 18S rRNA prolong the dwell time of 80S ribosomes at stop codons in a manner impeded by Rps26 in the 40S subunit exit channel, which leads to the proper completion of termination and ribosome recycling and prevents spurious translation of 3'UTR sequences by one or more unconventional mechanisms.*
>
> *Strengths:*
>
> *The standard 80S and selective eRF1 80S ribosome profiling data obtained using EZRA-Seq are of high quality, allowing the authors to detect an enrichment for purine-rich sequences upstream of stop codons at sites where termination is relatively slow and ribosomal complexes are paused with eRF1 still engaged in the A site.*
>
> *Weaknesses:*
>
> *There are many weaknesses in the experimental design, interpretation of results, and description of assay design and assumptions, the data obtained, and the interpretation of results, all of which detract from the scientific quality and significance of this work. In fact, a large proportion of paragraphs in the text and figure panels present some difficulty either in understanding how the experiment or data analysis was conducted or what the authors wish to conclude from the results, or that stem from an overinterpretation of findings or failure to consider other equally likely explanations.*

We appreciate the reviewer's thoughtful evaluation and constructive suggestions. We recognize that our original description of the MPRA and reporter assay results may have lacked sufficient clarity, particularly regarding the sequence motifs associated with termination pausing. In the revised manuscript, we have carefully rewritten these sections to clarify the experimental design, data interpretation, and relationship between sequence context and termination dynamics. We believe these revisions address the reviewer's concerns and improve the overall clarity of the manuscript.

> ***Reviewer #3 (Public review):***
>
> *Summary:*

This study from Jia et al carried out a variety of analyses of terminating ribosomes, including the development of eRF1-seq to map termination sites, identification of a GA-rich motif that promotes ribosome pausing, characterization of tissue-specific termination dynamics, and elucidation of the regulatory roles of 18S rRNA and RPS26. Overall, the study is thoughtfully designed, and its biological conclusions are well supported by complementary experiments. The tools and datasets generated provide valuable resources for researchers investigating the mechanisms of RNA translation.

Strengths:

(1) The study introduces eRF1-seq, a novel approach for mapping translation termination sites, providing a methodological advance for studying ribosome termination.

(2) Through integrative bioinformatic analyses and complementary MPRA experiments, the authors demonstrate that GA-rich motifs promote ribosome pausing at termination sites and reveal possible regulatory roles of 18S rRNA in this process.

(3) The study characterizes tissue-specific ribosome termination dynamics, showing that the testis exhibits stronger ribosome pausing at stop codons compared to other tissues. Follow-up experiments suggest that RPS26 may contribute to this tissue specificity.

Weaknesses:

The biological significance of ribosome pausing regulation at translation termination sites or of translational readthrough, for example, across different tissue types, remains unclear. Nevertheless, this question lies beyond the primary scope of the current study.

We thank the reviewer for the positive assessment of our work. We agree that tissue-specific differences in termination pausing were insufficiently described in the original submission. In response, and in light of similar concerns from other reviewers, we have expanded the relevant sections in the main text and Discussion. We now more clearly articulate both the biological context and the current limitations, identifying tissue-specific regulation of termination as an open question and future research direction.

Reviewer #4 (Public review):

Summary:

This manuscript by Qian and colleagues utilizes ribosome profiling, and reporter assays to dissect translation termination. Unfortunately, the data do not support the conclusions of the paper, controls are missing and several assays are not well validated and do not reproduce previous findings from others.

Specific comments:

Translation termination has been studied in several organisms including mammalian cells and yeast. In those cases what is analyzed is not the peak height at the stop codon, but rather the difference in the ribosome density before and after the stop. Thus, analyzing peak height is not validated. I understand that this is relevant only for the ribosome profiling experiments (and Ezra-seq) not the RF1 profiling. But much of the data was acquired that way.

Moreover, the data do not reproduce previous findings and no effort is made to connect them to previous data. Previous data has shown that stop codon efficacy varies. This is not reproduced (S1C). Similarly, an effect from the +1 residue is not reproduced. The data isn't even stratified by different stop codons as previous work has shown that different surrounding residues have different effects in the context of different stop

codons. Thus, none of the sequencing data is validated or trusted and does not reproduce previous findings.

The GA-rich sequence identified by Ezra-Seq and RF1 seq is not the same and it differs from previous sequences (Wangen &Green).

The authors claim that the majority of Rf1 peaks is at stop codons, but that is not true. It is only about 30% of the peaks. Also, not all mRNAs have peaks at the stop codons. That is at best problematic. Finally, there are mRNAs that are known to "suffer" from NMD, what do these look like in the Ezra-Seq and RF1-Seq? How about mRNAs that have programmed frameshifts? This raises questions on the validity of the eRF1 data.

Figure 4: First, instead of M/P ratio, one should analyze M/M+P, to normalize out differences in the loading and effects from collisions, which are guaranteed to occur here, but not considered or analyzed. Second, the data are analyzed as if what matters are codons in the P and E site (and beyond, where there are definitely NOT recognized codons). While there is evidence for some interactions, one would think that an additional analysis based on sequence would be helpful. Also, the supplemental data indicates that very rarely are there reciprocal changes (as should be the case), and as seen for stop codons.

Regarding the HiBit reporter assay: The two sequecnes clearly have effects on translation without considering stop codon context (Figure 4C), which need to be taken into account. Also, the effect from the sequences varies in the context of the assay in 4C and 4D (2-fold vs .5 fold), further questioning the assay. Moreover, the authors claim that re-initiation cannot account for Hibit levels, but that is clearly incorrect. The western in Figure 4E does not reproduce the data in 4D. While Hibit goes up (as in 4D, the putative GFP-fusion goes down. Finally, while the second reading frame should be more efficient is not explained and further argues for an artifact. Previous work (and work herein) suggests that read-through occurs equally in each reading frame. No controls for these assays are presented: e.g. stimulation by antibiotics, ABCE1 depletion, etc.

Figure 5 has similar problems. I don't understand how the Figure in 5A is made, but when you overlay the cited structures on Rps26, the molecules are identical. I guess the authors used some fantasy to build non-existing sequences differently into the structure. There is no basis for that. In panel C and the same in Figure 7, the number of analyzed mRNAs varies. This could influence the outcome and the EXACT same set of mRNAs should be analyzed. But the main problem here is that the authors need to analyze readthrough and not peak height as detailed above. Essential controls are missing that show what fraction of the 18S rRNA is mutated. Previous work has shown that 2 nt truncated 18S rRNA is actively degraded. It is hard to believe how 15% of altered ribosomes can abolish 100% of the effect from the C-rich sequences. Important validation is missing: the authors should analyze rRNA sequences in their ribo-seq dataset to demonstrate that they have the mutated rRNAs, and that these enrich and de-enrich as predicted.

In Figure 5-7 the authors develop a model that the sequence selectivity arises from base pairing between 18S rRNA and the mRNA. If so, then they should really stratify the data by number of WC pairs that can be formed. And only WC pairs, as GU pairs have a totally different geometry that will likely be discriminated against in this context. Also, the mutation is in a part of the helix that has no effect (Figure S3G). Thus, the data within the manuscript are inconsistent.

Figure 6 does not agree with published data (Li et al., Nature 2022). Previous work did not show testis-depletion of Rps26 in purified ribosomes. This is the critical difference as the authors here did not purify ribosomes. Also, another Rps is an essential control, even

> *if purified ribosomes are used. The validity of this dataset is thus questionable . Depletion from polysomes is hard to believe, as overall there is less signal in the polysomes.*
>
> *Figure 7 has similar problems as figure 5. Different pools of mRNAs are analyzed; peak height is not validated. Overexpression of Rps26 is not shown, as only Myc is shown, not Rps26. Beyond that, increased occupancy in ribosomes needs to be shown for the effect to come from ribosomes. Given how sick the cells are it is most likely that all effects are secondary and arise from whatever else is going on in the overexpression or depletion of Rps26. No controls are presented to show specific effects from Rps26.*
>
> *The authors need to check Rli1/ABCE levels in their cells. Their data have features that are indicative of low ABCE1 levels. These include a very small effect from ABCE1 depletion. These could be responsible for some of the effects they observe.*

We appreciate the reviewer's engagement with our study and the opportunity to clarify several points.

With respect to perceived inconsistencies with prior literature, we emphasize that our findings do not contradict established principles of translation termination. Rather, enabled by the development of eRF1-seq, we provide higher-resolution insight into termination dynamics that extends existing models. We have revised the manuscript to better contextualize our findings within prior studies and to avoid overstating novelty where continuity exists.

Regarding the analysis of ribosome profiling data, we note that peak height and read density are widely used metrics for inferring ribosome dwell time and pausing. Nevertheless, we recognize that our original presentation may not have sufficiently explained this analytical framework. In the revised manuscript, we have clarified the rationale and interpretation of peak-based analyses, particularly in Figures 5 and 7 involving 18S rRNA mutants and Rps26 perturbation.

Finally, we appreciate the reviewer's comments concerning base pairing. We have carefully revised both the Results and Discussion sections to present mRNA–rRNA interactions as a supported but not definitively proven mechanistic model, clearly distinguishing experimental evidence from inference.

We are grateful for the reviewers' thoughtful feedback. We believe the revisions have strengthened the manuscript by clarifying interpretations, moderating mechanistic claims, and expanding discussion of tissue-specific regulation, while preserving the central contributions of the study.

> ***Recommendations for the authors:***
>
> ***Reviewer #1 (Recommendations for the authors):***
>
> *(1) Some minor typos are present in the main text and methods section.*

We thank the Reviewer's attention to detail in reviewing our manuscript. We have now thoroughly revised the main text and methods section.

> *(2) S1I is missing or unlabelled.*

We are glad to have this opportunity to fix this mistake. Both S1I and S5D have now been added to the revised figures.

> *(3) Could the authors clarify in the main text whether crosslinking was a step in the eRF1-seq protocol? Pg 5: "Without crosslinking, ribosomal proteins were minimally pulled down by the eRF1 antibody, confirming the transient nature of eRF1 binding."*

Yes, crosslinking is needed for eRF1-seq. We tried no-crosslinking but very little was pulled down, as stated in the sentence in Page 5.

> *(4) Are termination events in the 5'-UTR or the CDS, as seen in the eRF1-seq data, also influenced by the GA-rich sequence? If the data is disaggregated into those two buckets, can you still pull out the motif?*

Yes, stop codons in 5'UTR and CDS share the same feature. However, the number of 5'UTR stop codons captured by eRF1-seq are too few to generate reliable sequence motif analysis.

> *(5) Could the authors please clarify what peaks/fractions they are using as the monosome in Figure 4A? From the manner in which the red boxes are drawn on the sucrose gradient profile traces, it seems that the 40S, 60S, 80S monosome and half of the disome peak are included in the monosome fraction.*

The red box shown in Figure 4A is a bit misleading. For the massive paralleled reporter assay, we selected ribosome fractions based on the sucrose gradient tracing corresponding to monosome and polysomes, respectively. However, the fraction accuracy is not absolute as the fraction tube corresponding to monosome could contain traces of subunits as well as disomes. In practice, 40S and 60S are less concerned than disome, but the primary component is 80S ribosome.

> *(6) On page 13, please cite references for Normal mode analysis.*

Normal Mode Analysis (NMA) using the Anisotropic Network Model (ANM) is a computationally efficient method for predicting large-scale, functional, and directional protein motions near equilibrium. We have followed the Reviewer's suggestion by citing a review paper in the field of structural biology (Bahar, I. et al. 2005).

> ***Reviewer #2 (Recommendations for the authors):***
>
> *(1) The authors interpret the height of RPF peaks at stop codons in their Ribo-Seq data as an indication of pausing by ribosomes during termination, resulting from slow or inefficient decoding of the stop codon and peptide release; although it could equally result from slow recycling of the 60S subunit by ABCE1 following peptide release. Arguing against the latter possibility, they show later in the study that shRNA knockdown of ABCE1 has little effect on the stop codon RPF peaks; however, because the ABCE1 depletion does not elicit collisions near the stop codon in the manner observed in other studies, it appears that the ABCE1 depletion was insufficient to impair recycling substantially. The authors also don't attempt to support their interpretation by showing that depletion of eRF1 increases the stop codon peaks and produces collisions just upstream of the stop codon. They never specify with any precision whether it is stop codon recognition by eRF1, peptide hydrolysis, or recycling of the 60S subunit from the post-termination complex that is delayed, which is very unsatisfying.*

We agree with the Reviewer that the RPF density at stop codons only reflects the dwell time of terminating ribosomes. In fact, it is not possible to dissect molecular details from Ribo-seq data sets, same as interpreting other pausing events. Regarding ABCE1, we did observe the increased termination peak in cells with ABCE1 knockdown (Figure S4C). The lack of collisions is perhaps due to incomplete depletion of ABCE1. Notably, ABCE1 depletion selectively increased ribosome density at the –15 nt position, whereas the forward-shifted –12 nt peak was largely unaffected (Figure S4D). These results suggest that ABCE1 primarily facilitates late-stage termination or ribosome splitting, and its absence delays pre-termination progression. Nevertheless, the main focus of the study is to decipher the sequence context of termination pausing, which seems to be irrelevant to ABCE1. We thank the Reviewer for understanding.

> *(2) They found enrichment for a GA-rich motif in the mRNAs with the largest stop codon peaks, which they attribute to its effect in slowing down some aspect of termination or ribosome recycling to increase the dwell time of the terminating ribosomes. They found no motif, however, in mRNAs containing the smallest RPF peaks at stop codon peaks, which presumably terminate more rapidly; even though they conclude later in the study from their massively parallel reporter assays (MPRA) that "C-richness" in the 9 nt 5' of stop codons enables rapid termination. The mRNAs with high pause scores at the stop codon that are enriched for the GA motif also show lower RPFs in 3'UTRs compared to the low pause score mRNAs, which they interpret to mean that long-lived termination complexes produce more efficient peptide termination and ribosome recycling, while short-lived complexes fail to be recycled and continue translation into the 3'UTR. However, because the 3'UTR reads are in all three frames, this could not occur simply by stop codon readthrough but would also require a frameshift upstream or at the stop codon itself to prevent termination and continued translation into the 3'UTR; and it could also arise from unconventional reinitiation by unrecycled post-termination complexes, which has been seen by others on inhibition of 60S recycling. The authors' interpretation is too simplistic.*

We thank the Reviewer's summary about the sequence features controlling ribosome dwell time at stop codons uncovered by eRF1-seq. We are fully aware of the complex scenarios about 3'UTR translation, however, unconventional reinitiation cannot explain the results of the reporter assay shown in Figure 4D. Unlike frameshifting that generates prolonged products with mixed C-termini, reinitiation is associated with a new start. In Figure 4D, we observed products with C-terminal fused HiBiT, which cannot be explained by reinitiation. We thank the Reviewer for understanding.

> *(3) They obtain support for the role of a GA-motif in pausing at stop codons from their selective ribosome profiling of eRF1-bound 80S ribosomes present at stop codons, finding a related GA-motif enriched at stop codons with high occupancies of eRF1-bound RPFs. However, once again, there is no C-rich motif enriched upstream of stop codons with low eRF1-bound RPF occupancies, at odds with later claims for such a motif. They ultimately propose that the GA motif pauses terminating ribosomes by base-pairing with the 3' end of 18S rRNA in the ribosome mRNA exit channel, principally utilizing two UU residues at the penultimate bases in the 18S rRNA that presumably base-pair with either A or G residues in the GA motif.*

The Reviewer might be confused by the results from Ribo-seq and massively paralleled reporter assay (MPRA). Ribo-seq data sets are limited to endogenous sequences that were shaped during evolution. In contrast, MPRA uses completely randomized sequences that offer unbiased analysis of sequence elements. The lack of C-rich motif in eRF1-seq data sets is due to the under-representation of such sequence elements in human genome. Perhaps this sequence bias is beneficial for termination fidelity by minimizing 3'UTR translation. We have further clarified this point in the revised manuscript.

> *(4) They claim to have obtained independent confirmation of this last idea from their massively parallel reporter analysis (MPRA), in which sequences upstream of the stop codon of a uORF were randomized to determine those that appear to prevent translation downstream of the uORF and thereby place the mRNA in the monosome fraction versus those that allow downstream translation by any mechanism including leaky scanning of the uORF start codon, stop codon readthrough, or reinitiation (the assay doesn't distinguish between these mechanisms) and place the mRNA in the polysome fraction. In actuality, their results showed that the presence of only GGG triplets at any location in the 9 nt substantially prevents downstream translation, whereas only CCG and CCC proline codons enable downstream translation by one or more mechanisms. In view of their final model, it's very difficult to understand why GGG at any position would be able*

> *to base-pair with the U-U residues in the 18S rRNA when the stop codon is in the A site, and also why the many other triplets with two G's, two A's or an A and G base-all consistent with the GA-rich motif identified earlier-would not act similarly. Similarly, it's also puzzling that CCG and CCC can exert their effects at multiple positions upstream of the stop codon, and why the 7 other codons with two C's do not act similarly. Thus, it's unconvincing that a specific C-rich motif (which they refer to repeatedly but never identify) or even C-richness upstream of the stop codon confers elevated downstream translation. It's also important to note that the MPRA does not report on pausing at stop codons explicitly, only on whether ribosomes can be found downstream of the uORF stop codon, and assigning this outcome to the presence or absence of pausing during termination requires an ad hoc assumption that the authors have not identified as such.*

The Reviewer brought up excellent points in this comment regarding the MPRA result. Indeed, MPRA does not report ribosome pausing events as pointed out by the Reviewer. Additionally, MPRA is not designed to distinguish mechanisms underlying translational readthrough. As we mentioned above, both MPRA and Ribo-seq bear different experimental features that partly explain the similar, but not identical sequence motif uncovered by two assays. The prominent GGG motif identified by MPRA is intriguing, reminiscent of our prior study focusing on translation initiation (Jia et al. NSMB 2020). We propose that G-rich sequences upstream of stop codons form G-quadruplexes that block ribosome movement, resulting in monosome enrichment. Supporting this notion, the GGG motif was not identified by eRF1-seq, echoing the importance of using complementary experimental procedures in drawing conclusions.

> *(5) They claim to confirm their conclusions from the profiling and MPRA data by measuring translation of the HiBiT sequence inserted downstream of the stop codon of the uORF in two reporters in which the upstream 9 nt contain either a single C-rich sequence or a single G-rich sequence. It's unclear how or why these two particular sequences were chosen. The G-rich sequence does not conform closely to either of the GA-motifs captured in the sequence LOGOs of Figures 1-2, and as noted above, there was no C-rich motif ever identified in these analyses. Thus, it's unclear whether the different effects of these two sequences are representative of sequences that pause or do not pause terminating ribosomes that they identified by the genome-wide analyses. In addition, given that the exact position of the GG or CC sequences relative to the stop codon doesn't seem to matter based on the MPRA data, it is actually possible to find the same number of base pairs with the 3' end of 18S rRNA for both of the two GA-rich and C-rich sequences analyzed in these reporter assays by sampling different registers of pairing between the mRNA and 18S rRNA. What is needed instead is be a systematic analysis using both the polysome:monosome assay, and the HiBiT translation assay of sequences that can pair perfectly with the 18S rRNA or contain increasing numbers of mismatches predicted to destabilize the putative helix that would be formed, and to determine whether the stability of the helices thus formed is highly correlated with the presence of the reporter mRNA in monosomes and with low HiBiT translation.*

We appreciate the Reviewer's effort to improve our manuscript. The sequences inserted into the reporters were chosen based on several considerations. First, we chose the GA-motif rather than the G-rich sequences because the former represents physiological sequence element uncovered by eRF1-seq. As mentioned above, the G-rich sequences could form G-quadruplex artifacts. Second, the C-rich sequences were uncovered by both eRF1-seq (Figure 2D) and MPRA (Figure 4b). Third, only sequences top ranked were selected for the reporter assay. For the positional effects of inserted sequence elements, it is important to note that the proposed mRNA:rRNA interaction is not static because of the continuous mRNA movement along the channel. Instead of using sequences with perfect pairing, we have conducted experiments by placing the C-rich sequences at different positions of the insert. As shown in

Figure S3H, the position relative to the stop codon does not seem to matter. In the revised manuscript, we have rephrased several sentences in the main text to avoid confusion.

> *(6) They attempt to support their model by overexpressing a mutant 18S rRNA with mutations of the penultimate U-U residues to G-G, and present evidence that this decreases the stop codon RPF peaks on mRNAs rich in GA sequences upstream of the stop codons, and has the opposite effect on mRNAs that are C-rich; however, they never indicate the criteria used to assign mRNAs to these two bins, and whether it is based on the GA-rich motifs/LOGOs identified by genome-wide analysis or on the few triplets turned up by the MPRA. Clearly, it would be far better to conduct the same analysis of motif enrichment for high and low pause scores that produced the motif in Figure 1C and determine if the motif for high pausing switches from the GA-rich motif for WT 18S rRNA to a C-rich motif for the mutant, and vice versa for the low pause score mRNAs. It should also be noted that the C-rich sequence used in the reporter can form only 2 base pairs with the mutant 18S rRNA when the mRNA's C-C dinucleotide base pairs with the new G-G dinucleotide in rRNA, but it can actually form 4 base pairs with the WT 18S rRNA sequence in a different pairing register, undermining their interpretation of these data. Note also that there was no analysis done to determine what proportion of 40S subunits actually contain the mutant 18S rRNA, which is expected to be only a minor fraction under the best circumstances, and cannot simply be taken for granted, requiring a direct analysis of the sequences of the 3' ends of 18S rRNA in the cells expressing the mutant 18S.*

The Reviewer's comment on 18S rRNA mutants are insightful. Given the low percentage of ribosomes incorporated with the rRNA mutants, it is not feasible to conduct motif analysis based on ribosome pausing at stop codons. As shown in Figure 5C, stop codon peaks are still evident after 18S mutant transfection albeit less prominent than the wild type. Notably, introducing 18S rRNA mutants into cells is not an easy task, and we have followed closely the protocol published previously (Burman and Mauro. NAR 2012) to obtain meaningful data. We believe (and hope the Reviewer will concur) that the experiment using the 18S rRNA mutants offers critical evidence in support of the mechanism.

> *(7) They attempt to implicate Rps26 in the pausing by depleting or overexpressing (OE) the protein and comparing pausing at stop codons between the same two ill-defined GA-rich and C-rich bins of mRNAs mentioned above and by assaying the HiBit reporters. Again, they haven't determined whether the amount of Rps26 in mature 40S subunits is reduced or elevated compared to WT cells, and their interpretation of the OE data actually depends on the occurrence of 40S subunits lacking Rps26 in unstressed WT cells, which seems improbable and requires direct confirmation. Also, they haven't quantified the 80S peaks at the stop codons relative to the CDS reads immediately 5' of the stop codons, which varies with Rps26 OE versus the WT control, and doing so might well contradict their conclusion. Moreover, the C-rich and GA-rich HiBiT reporters behave identically rather than oppositely in response to Rps26 OE, which the authors fail to acknowledge or comment on.*

The Reviewer might be confused by the role of Rps26 partly due to the lack of clarity in our original description of the results. In yeast, Rps26 can dissociate from fully assembled 80S ribosomes under stress (Yang, et al. Sci Adv 2022). Therefore, although quantifying the Rps26 in mature 40S subunits is informative, it does not infer the composition of 80S ribosomes in cells with Rps26 depletion or overexpression. As pointed out by the Reviewer, we also noticed that, in cells with Rps26 depletion or overexpression, mRNAs with C-rich sequences showed no difference of ribosome density at stop codons. This is quite expected because C-rich sequences have minimal interaction with the 3' end of rRNA. As a result, Rps26 depletion or overexpression is not supposed to affect ribosome dwell time at stop codons with upstream C-rich sequences. In contrast, only stop codons preceded with GA-rich sequences are influenced

by Rps26 heterogeneity. In the revised manuscript, we have clarified this confusion in the main text.

> *Additional specific comments*
>
> *(8) In the Summary statement: "We identify a sequence motif upstream of the stop codon that contributes to termination pausing, which was confirmed by massively paralleled": This is unjustified, as the MPRA showed only that a GGG triplet inserted anywhere in 9 nt 5'of the stop codon reduces ribosomes from traversing a stop codon either by blocking leaky scanning or reinitiation after an upstream uORF, and it is unclear why the position of this triplet does not matter nor why other GA-rich sequences capable of base pairing with the 3' end of 18S rRNA were not identified in the MPRA.*

As mentioned above, eRF1-seq and MPRA assays are complementary with advantages and disadvantages. Nevertheless, the Reviewer's comments are well-taken and we have rephrased the Abstract of the revised manuscript.

> *(9) A supplementary figure explaining EZRA-Seq would be very helpful.*

Since EZRA-seq methodology has been published (Mao, et al. NSMB 2023), we think a citation makes more sense. We thank the Reviewer for understanding.

> *(10) The bottom plots/histograms of Figure 1A are very unclear. What is the y-axis of the bottom histogram, and relative to what elongating ribosomes have been analyzed?*

We apologize for the confusion in the histograms of Figure 1A. We stratified all mappable reads into footprints of initiating, elongating, and terminating ribosomes. Like many Ribo-seq results, the majority of footprints are of 29 nt length. If all three ribosome groups are of the same conformation, they are expected to have the same size distribution of the footprint length with the same bar height. It is true for initiating ribosomes (left) but not terminating ribosomes (right). We have now rephrased the figure legend in the revised manuscript.

> *(11) Page 5: "A close inspection of stop codon footprints revealed an additional peak at -12 nt, which becomes more prominent when the reads are shorter (Figure 1B)." No explanation is offered for this finding. Do forward-shifted termination complexes have an empty A site owing to dissociation of eRF1? If so, they would be undetectable in eRF1-Seq data.*

Previous toe-printing assays have shown that eRF1 induces a forward movement of terminating ribosomes, shifting the leading edge from +13 nt to +15 nt (Pisarev, et al. Cell 2007). Moreover, single-molecule analyses have identified distinct pre- and post-termination phases catalyzed by eRF1 (Lawson, et al. Science 2023). Together, these observations suggest that the two 5' end peaks correspond to pre- and post-terminating ribosome states, with the latter likely adopting a rotated conformation. We have revised the relevant paragraph in the main text.

> *(12) Page 5: ". It is possible that the two distinct 5' end peaks represent pre- and post-terminating ribosomes, with the latter assuming the rotated conformation. We could not rule out the possibility that these terminating ribosomes have the stop codons at the P-site prior to disassembly." The logic here is difficult to follow.*

We have revised the relevant paragraph in the main text.

> *(13) Figure 1C: provide coordinates relative to the stop codon on this motif.*

The motif analysis is position-independent and there is no coordinate on the logo plot.

> *(14) Page 6: "This was not due to biased downstream sequences as the +4 nucleotide minimally affected the 3'UTR translation (Figure S1C)." The logic here is unclear.*

We have rephrased this sentence to “This effect could not be explained by downstream sequence bias, as the identity of the +4 nt had minimal impact on 3’UTR translation (Figure S1C).”

> *(15) Page 6: "Like Ribo-seq, we also observed a forward shifting of post-terminating ribosomes from eRF1-seq (Figure 2C). " But by definition, they will have eRF1 in the A site, so why are they 26nt vs 29nt?*

Like many Ribo-seq results, the majority of footprints are of 29 nt length. However, ribosome populations with smaller footprint sizes are of physiological meanings, likely due to conformation changes.

> *(16) Page 6 "In agreement with the Ribo-seq data sets, eRF1-seq revealed that not all the mRNAs exhibited eRF1 peaks at the annotated stop codons (Figure 2B), echoing the wide range of termination pausing." It should be determined whether eRF1 occupancy is correlated with 80S occupancy at stop codons in the standard Ribo-Seq. And if not, why?*

As shown in Figure 2B, there is a strong correlation between eRF1-seq and Ribo-seq in terms of termination pausing. However, the pausing index will be different between these two data sets due to distinct normalization. We thank the Reviewer for understanding.

> *(17) Figure 2D: The plot on the left doesn't specify how far upstream the triplets can be from the stop codon. Is the LOGO significantly more similar to that shown in Fig. 1C than expected by chance alone?*

In Figure 2D, the codon frequency analysis is position independent. Similarly, the sequence logo in Figure 1C and Figure 2D is also position independent.

> *(18) Page 7: ". Notably, three different stop codons show similar pausing features and sequence motifs (Figure S1G and S1I)." The figure citations here are incorrect.*

We apologize for the missing Figure S1I, which was also pointed out by Reviewer #1. We have now updated Figure S1 in the revised manuscript.

> *(19) Page 7: The term "false termination" is a poor descriptor if termination doesn't occur.*

We have followed the Reviewer’s suggestion by replacing “false termination” with “failed termination”.

> *(20) Page 8: "Consistent with previous reports 27, mutating the stop codon UAG abolished the reinitiation event that drives out-of-frame HiBiT translation (Figure 3E)." How is HiBit assayed? No details are given in the legend. This result doesn't confirm any of the actual eIF1 peaks upstream of stop codons, just that REI can occur at some level 5' of stop codons; and the eRF1 peak at the HiBit stop codon would be 3' of the peak at the main stop codon.*

HiBiT assay is a standard reporter like luciferase and Promega offers a detection kit, as described in the methods section. The result shown in Figure 3E is to confirm stop codon-associated reinitiation, which suggests that ribosomes migrated from the stop codon could contain eRF1 before reaching a start codon for reinitiation. We have revised this paragraph to avoid confusion.

> *(21) Figure 4A: Unclear what position 0 to 6 in the bottom heat map corresponds to in the inserted 9 nt sequences. Are these codon positions vs. nucleotide positions? The*

> *legend lacks explanatory information.*

Figure 4A shows nucleotide positions (x axis) grouped by 3nt to reflect codon information (y axis). For the inserted 9nt random sequences, the last two nucleotides cannot be used because of the fixed nucleotides downstream of the insert. The same analysis has been reported in our prior study (Jia, et al. NSMB 2020).

> *(22) Page 8: "For instance, codons enriched in frame 2 belong to NUA and NUG, another indication of in-frame stop codons (Figure S3B, bottom panel). " Need more or better explanation here.*

We have rephrased this sentence in the main text. “Codons enriched in alternative reading frames were also informative; for example, codons enriched in frame 2 predominantly belong to NUA and NUG, consistent with frameshifted presentations of in-frame stop codons (Figure S3B, bottom panel).”

> *(23) "This is likely due to the faster turnover of these mRNAs because of 3'UTR translation". Need more or better explanation here.*

MPRA in Figure S3C showed that mRNA variants containing C-rich downstream sequence were depleted from both monosome and polysome fractions. Since 3’UTR translation is well-established to induce mRNA decay, it is possible that these sequences are under-represented due to mRNA turnover. We have added more explanations in this paragraph in the revised manuscript.

> *(24) " Figure 4B: The logic and assumptions of this assay are not explained. How do ribosomes traverse the uORF, by leaky scanning or by stop codon read-through that is impeded by a ribosome stalled at the uORF stop codon? Presumably, it can't be read through as the uORF is out of frame and translation would likely terminate quickly.*

The rationale of Figure 4B is very similar to Figure 4A, except for the presence of the stop codon UAG. Under efficient termination, a monosome enrichment is expected, which could be promoted by termination pausing or structural hinderance by G-rich sequences. In contrast, stop codon readthrough or reinitiation would lead to polysome enrichment. We have thoroughly revised this paragraph in the main text.

> *(25) Figure 4B results: It's unclear why M/P ratios are so low in Figure 4B vs Figure 4A as all constructs in 4B contain a stop codon and should have the high M/P ratios seen for the constructs in panel (A) with stop codons inserted. It's also unclear why the high M/P ratio should be so limited to GGG triplets vs. other triplets that conform to the GA-rich motifs identified above, and also why this triplet would not function at codon position 6. Similarly, it's unclear why only CCG and CCC and not CCU and CCA have an effect, and why only 3 of 9 codons with 2 or more C's have the effect, all suggesting that specific sequences and not just C-rich sequences are promoting read-through. Yet, no C-rich motif was discernible in the profiling experiments above.*

We appreciate the Reviewer’s careful reading of our manuscript. In profiling experiments shown in Figure 2, we did observe C-rich codons albeit with variations. Possible reasons include sequence differences between human genome and randomized sequence combinations. In addressing the Reviewer's question 23, we have thoroughly revised this paragraph in the main text.

> *(26) Page 9: "These results are in line with the sequence specificity in termination pausing revealed by Ribo-seq and eRF1-seq." This is unjustified as the results in 4B are restricted to only GGG triplets rather than numerous triplets that equally conform to the AAGAAGA motif defined above.*

We apologize for the overstatement in this sentence. In addressing the Reviewer's question 23 and 24, we have thoroughly revised this paragraph in the main text.

> *(27) Page 9: "This result is congruent with the MPRA assay, suggesting that the C-rich coding sequence preceding the stop codon not only reduces termination pausing, but also promotes downstream translation." This is unjustified as the single C-rich sequence chosen for the analysis in Figure 4C is not representative of the two C-rich triplets identified in Figure 4B, showing strong evidence of read-through.*

In Figure 4C, both C-rich and GA-rich sequences were chosen from shared elements between eRF1-seq and MPRA as they represent physiological sequences associated with termination pausing. The reporter assay is crucial in linking the lack of termination pausing with 3'UTR translation. We thank the Reviewer for understanding.

> *(28) The analyses in Figures 4C-D suffer from a lack of the no-stop codon controls to allow the standard quantification of read-through as a percentage of continuous translation in the zero frame in the absence of a stop codon.*

The Reviewer might have missed the no-stop codon control in Figure 4C, which contains reporters with (bottom) and without (top) UAG stop codon. In Figure 4D, it is not feasible to include no-stop codon control for frameshifting reporters as the HiBiT value will be out-of-chart several orders of magnitude.

> *(29) Page 10: "Therefore, the C-rich coding sequence triggers ribosome sliding at the stop codon, resulting in 3'UTR translation in all three reading frames." Sliding is an imprecise term. It is presumably a stop codon readthrough accompanied by frameshifting.*

We agree with the Reviewer's suggestion and have replaced the word of "sliding" with "readthrough".

> *(30) Page 10: The citation to Figure S3H is incorrect, as there is no panel H.*

We are glad to have this opportunity to fix this error. We have now added panel H into the Figure S3 in the revised manuscript.

> *(31) Page 10: "When the ribosome occupancy in the CDS was normalized, loss of ABCE1 led to a modest increase of stop codon peaks (Figure S4C)". Is this increase reproducible in replicates and statistically significant, as it seems very slight?*

The increased ribosome peak at stop codons in cells lacking ABCE1 is not significant, partly due to incomplete depletion of ABCE1 as shown in Figure S4A. Since ABCE1 is not the focus of this study, we did not attempt to knock out ABCE1, which could cause cellular toxicity.

> *(32) Page 11: "Notably, the elevated ribosome density occurred at all stop codons, an indication of global effects." Where are the data substantiating this claim?*

We apologize for the confusion here. In the revised manuscript, we have deleted this sentence from the main text.

> *(33) Page 11: "A closer look revealed that silencing ABCE1 increased the ribosome density at the -15 nt position". This claim is not convincing in the 29 nt read data, where it should be observed.*

We agree with the Reviewer that the increased ribosome density at the -15 nt position is more evident for shorter footprints. We have revised the sentence in the main text.

> *(34) Page 11: "Since the 3' end of 18S rRNA contains a highly conserved U-rich sequence (GAUCAUUA), the GA- rich sequence element of mRNA could follow U:A and U:G base*

> *pairing near the exit site" (Figure 5A and S5A). By contrast, the C-rich sequence motif on mRNA would escape the 18S rRNA checkpoint, resulting in faster mRNA passthrough." This seems simplistic, as there would also be three G-A or A-G mispairings with 18S rRNA at other positions of the (G/A)AAGAAGA motif. Also unclear what the C-rich motif actually is, making it impossible to determine how many pairings it could make with the 18S rRNA sequence.*

Unlike base pairing on RNA structures, the putative rRNA:mRNA interaction is dynamic because of the continuous movement of mRNA along the ribosome channel. In fact, perfect base pairing might not be instrumental. Therefore, the difference between GA-rich and C-rich sequences is reflected in the accumulated effect. As mentioned above, the C-rich sequences are derived from both eRF1-seq and MPRA.

> *(35) Figure S5B: Showing this sequence is misleading. While not described, it is presumably the DNA sequence of the plasmid, not the rRNA sequence, as there is 100% of the mutant sequence. They need to sequence the 3' end of rRNA isolated from ribosomes to confirm the presence of mutant ribosomes at appreciable levels.*

The Reviewer is correct that the sequences shown in Figure S5B are from the plasmids. To avoid such confusion, we have removed the sequences in the updated Figure S5B.

> *(36) Page 12: "When mRNAs are stratified based on the sequence motif upstream of stop codons, we found that overexpression of the 18S mutant reduced the differential termination pausing between GA-rich and C-rich sequences (Figure 5C)". It is not explained what GA-rich or C-richness means precisely. Moreover, the same kind of analysis done in Figure 1C should have been conducted here to determine the LOGOs for high and low pausing for WT vs mutant 18S rRNA.*

We understand why the Reviewer repeatedly ask about the GA-rich and C-rich sequences, partly due to the lack of clarity in our original description of the analysis. The GA-rich transcripts were defined as those have the upstream 15-nt sequence with G or A nucleotides more than 65% (9 nt); whereas C-rich transcripts were defined as those with C more than 40% (6 nt). We have now updated the methods section in the revised manuscript.

> *(37) Page 12: "Notably, the 3' end sequence of 18S rRNA is highly conserved (Figure S5D)". There is no Figure S5D in the figures.*

We are glad to have this opportunity to fix this error. We have now added panel D and E into Figure S5 in the revised manuscript.

> *(38) Page 13: "Further supporting the sequence specificity of termination pausing, testis mRNAs with prominent stop codon peaks are enriched with GA-sequences upstream of the stop codon (Figure S6C). The same group of mRNAs, however, barely exhibit termination pausing in liver." Again, motif analysis of high and low pausing should have been done here.*

The motif analysis in mouse tissue samples is less informative because GA-rich sequences will be over-represented in testis, whereas the same group will be under-represented in liver. We had to select the shared mRNAs for comparative analysis. We thank the Reviewer for understanding.

> *(39) Page 13: "While liver exhibited a similar distribution of Rps26 and RACK1 in polysome fractions, testis showed an evident depletion of Rps26 in polysome (Figure 6C). Notably, a substantial amount of Rps26 is present in the ribosome-free fraction of testis." They failed to normalize Rps26 levels in polysomes for bulk polysome levels, as indicated by the A260 tracings to determine if polysomes are depleted of Rps26, or rather, there is less polysomal Rps26 simply because polysomes are less abundant.*

We agree with the Reviewer's notion regarding different polysome traces between testis and liver. Because the polysome volume is difficult to normalize, we used RACK1, a constitutive component of ribosome, to quantify the amount of polysome.

> *(40) Page 14: "Indeed, normal mode analysis (NMA) by anisotropic network models suggests that, in the absence of Rps26, both the -3 to -9 extension of the mRNA and the 3' end of 18S rRNA can twist and approximate to each other with improved mutual parity (Figure 7B)." It is unclear what this means.*

Normal Mode Analysis (NMA) by Anisotropic Network Model (ANM) is a coarse-grained computational method used to study biomolecular dynamics by modeling proteins as a network of nodes connected by springs. Unlike the Gaussian Network Model (GNM), ANM calculates the full 3D directional preference of motion, enabling characterization of conformational changes, domain movements, and flexibility in large macromolecules. We have added a citation (Bahar, I. et al. 2005) in the revised manuscript.

> *(41) Page 14: "To investigate whether Rps26 haploinsufficiency affects ribosome dynamics at stop codons, we knocked down Rps26 from HEK293 cells using shRNA (Figure S7A)". Haploinsufficiency properly refers to a heterozygous null/WT genotype, not shRNA knockdown.*

The Reviewer is correct in terms of haploinsufficiency. We have replaced the word of "haploinsufficiency" with "reduced Rps26 levels" in the revised manuscript.

> *(42) Page 14: "The reciprocal change echoes the tissue-specific differences in initiation and termination (Figure 6A). " It's unclear why these peaks should be reciprocally related mechanistically, so examining changes in their ratio may not be incisive. Rps26 KD could reduce the efficiency of termination independently of pausing. And does Rps26 KD affect eRF1 occupancies in parallel with 80S occupancies?*

A prior study reported that Rps26 regulates translation initiation by recognizing Kozak sequence elements (Ferretti, et al. NSMB 2017). We therefore speculate that the role of Rps26 in termination might be correlated, although we don't have direct evidence. We have further clarified this point in the discuss section of the revised manuscript.

> *(43) Page 14: "The increased termination pausing, once again, primarily occurs at stop codons preceded by GA-rich sequences (Figure 7C)". No statistical analysis of replicates was done to see if the increase is significant, as it is quite small. They could have stratified mRNAs according to the number of base-pairs they can form with 18S rRNA rather than using this nebulous GA-richness, and see if the conclusion still holds.*

The metagene analysis shown in Figure 7C is standard for comparison of ribosome footprint distribution. We agree that the increase of termination peak at stop codons preceded by GA-rich sequences is not as striking as it should be, this is an underestimate because only a small fraction of ribosomes have sub stoichiometry of Rps26.

> *(44) Page 14: "Remarkably, when mRNAs are stratified based on the sequence motif upstream of stop codons, we found that overexpression of Rps26 reduced the ribosome density (>50%) at stop codons preceded by the GA-sequence (Figure 7E)." They failed to normalize reads to the CDS occupancies to control for fewer ribosomes reaching the stop codons, especially considering that depletion of elongating 80S appeared to occur just upstream of stop codons on Rps26 OE. The same problem exists for the C-rich mRNAs. Also, their interpretation of the effects of Rps26 OE depends on there being Rps26-lacking 40S subunits in WT unstressed cells, which seems unlikely and has not been established directly. Finally, they didn't show increased Rps26 content in 40S subunits on Rps26 OE, which is also required.*

This question is the same as #7, which we have fully addressed in this letter (page 7).

> *(45) Page 15: "To affirm the mechanistic connection between stop codon pausing and termination fidelity, we conducted HiBiT reporter assays that showed increased 3'UTR translation in cells with Rps26 overexpression (Figure 7F)." But both the C-rich and GA-rich reporters show increased expression on Rps26 OE. Why should that be if the C-rich sequences don't base pair with 18S rRNA in WT cells and are unaffected by Rps26 depletion? These data suggest that some other mechanism underlies the increased expression of the GA-rich reporters seen on Rps26 OE.*

The Reviewer's concern is valid, and we agree that additional mechanisms might contribute to the increased reporter expression. The simplest explanation is that Rps26 overexpression promotes ribosome biogenesis, which globally increases mRNA translation. Supporting this notion, more polysome could be observed in cells with Rps26 overexpression (Figure S7E).

> *(46) Page 15: "Without pausing at stop codons, terminating ribosomes are likely to undergo incomplete dissociation, resulting in continuous translation in 3'UTR." The language here is imprecise. Are they proposing reinitiation by unrecycled 80S ribosomes, or stop codon read-through with or without frameshifting, or both?*

This question is the same as #2, which we have fully addressed in this letter (page 3).

> *(47) Page 15: "Importantly, lack of termination pausing leads to stop codon-associated random translation, giving rise to mixed C-terminal extension." Again, what does this mean? Read-through generally accompanied by frameshifting?*

Stop codon-associated random translation differs from ribosome readthrough, reinitiation, or frameshifting. We have extensively clarified this confusion in the revised manuscript.

> *(48) Page 16: "For terminating ribosomes, the prolonged dwell time at stop codons offers an extended window for eRF1 loading, peptide cleavage, and ribosome recycling." This sentence is confusing because the eRF1-Seq data suggest that the pause occurs after eRF1 decodes the stop codon, with delayed peptide cleavage and recycling.*

We thank the Reviewer's effort to improve our manuscript. We have rephrased the entire paragraph in the revised manuscript.

> ***Reviewer #3 (Recommendations for the authors):***
>
> *The manuscript is well-written, and the conclusions are overall well-supported by the data. I have only a few relatively minor questions and comments:*
>
> *(1) For termination sites overlapping with coding regions, the lack of 3-nt periodicity downstream of these sites could result from overlapping translation of multiple ORFs, rather than indicating that translation readthrough events can happen in multiple frames. Could the authors clarify this interpretation?*

We appreciate the Reviewer's positive comments on our manuscript. The Reviewer is correct that overlapping ORFs would result in the lack of 3-nt periodicity. Although it is common for overlapping ORFs near the canonical start codons, ORFs overlapping the canonical stop codons are rare. Nevertheless, we have rephrased the statement in the revised manuscript.

> *(2) The observation that multiple eRF1-seq peaks are located within CDS regions suggests that eRF1 may compete with A-site tRNAs during elongation. This is an interesting finding. Do the authors think this competition could lead to premature termination, or is it more likely to represent elongation pausing? Additionally, do the authors observe corresponding ribosome pausing peaks at these sites in conventional Ribo-seq data?*

The Reviewer's comment on eRF1-seq peaks in CDS is insightful. We agree that pre-mature termination is possible because of competition. However, we do not observe corresponding ribosome pausing peaks in regular Ribo-seq, presumably due to low frequency of which events.

> *(3) Regarding the regulation of ribosome pausing across tissue types, how robust are these results? For example, are the tissue-specific effects (such as stronger pausing in the testis) consistent among different mice or across age groups, given that many aspects of translational regulation are known to change with aging?*

We found that tissue-specific distribution of ribosome footprints is highly reproducible, especially liver and testis. Notably, the lack of termination peaks in liver is also reported by other independent studies (Gobert, et al. PNAS 2020), arguing that such effect is not a result of sequencing bias. We haven't compared mice with different ages, but aging-associated translational regulation is an interesting topic awaits further investigation.

> ***Reviewer #4 (Recommendations for the authors):***
>
> *(1) Translation termination has been studied by ribose in several organisms, including mammalian cells and yeast. In those cases, what is analyzed is not the peak height at the stop codon, but rather the difference in the ribosome density before and after the stop. Thus, analyzing peak height is not validated. I understand that this is relevant only for the ribosome profiling experiments (and Ezra-seq), not the RF1 profiling. But the large majority of the data was acquired that way.*

With due respect, we disagree with the Reviewer's point regarding how to study ribosome dynamics at stop codons. Comparing footprint density before and after stop codons does not infer dynamics of terminating ribosomes. By establishing eRF1-seq, we are for the first time able to analyze ribosome behaviors at stop codons, which represents a significant advancement of technological development.

> *(2) Moreover, the data do not reproduce previous findings, and no attempt is made to connect them to previous data. Previous data have shown that stop codon efficacy varies. This is not reproduced (S1C). Similarly, an effect from the +1 residue is not reproduced. The data isn't stratified by different stop codons, and previous work has shown that different surrounding residues have different effects in the context of different stop codons. Thus, none of the sequencing data is validated or trusted and does not reproduce previous findings.*

We are certainly aware of previous findings regarding stop codon readthrough. We would like to emphasize that our findings do not contradict established principles of translation termination. Rather, enabled by the development of eRF1-seq, we provide new insights into termination dynamics that extend existing models.

> *(3) The GA-rich sequence identified by Ezra-Seq and RF1 seq is not the same, and it differs from previous sequences (Wangen &Green).*

We don't quite understand why the Reviewer is preoccupied with prior studies without accepting new results obtained from newly developed technology. The GA-rich sequences identified by Ezra-Seq and eRF1-seq are similar, albeit not identical. This is simply because eRF1-seq offers much higher resolution to reveal termination pausing than regular Ribo-seq.

> *(4) The authors claim that the majority of Rf1 peaks are at stop codons, but that is not true. It is only about 30% of the peaks. Also, not all mRNAs have peaks at the stop codons. That is, at best, problematic. Finally, there are mRNAs that are known to "suffer"*

> *from NMD. What do these look like in the Ezra-Seq and RF1-Seq? How about mRNAs that have programmed frameshifts? The eRF1 data is invalid.*

The Reviewer is confused about the eRF1 peak density versus frequency, which has totally different meanings. Additionally, the Reviewer seems to be surprised that not all mRNAs have peaks at the stop codons. The differential ribosome dynamics at stop codons is an exciting feature previously unappreciated, rather than problematic. Regarding programmed frameshifting, we argue that such events are rare in mammalian cells.

> *(5) Figure 4 has many flaws; it is hard to know where to start. First, instead of the M/P ratio, one should analyze M/M+P, to normalize out differences in the loading and effects from collisions, which are guaranteed to occur here, but not considered or analyzed. Second, the data are analyzed as if what matters are codons in the P and E site (and beyond, where there are definitely NOT recognized codons). While there is evidence for some interactions, one would think that an additional analysis based on sequence would be helpful. Also, the supplemental data indicate that very rarely are there reciprocal changes (as should be the case), as seen for stop codons. Thus, the assay is at best questionable and likely worse.*

The Reviewer appears to be unfamiliar with massively parallelled assay, which has been widely used to uncover sequence elements crucial in translational regulation. We urge the Reviewer to read our prior study using MPRA to investigate alternative translation initiation (Jia, et al. NSMB 2020). The similar approach has also been used to decipher 5' UTR sequence elements in mRNA engineering (Sample, et al. Nat Biotech 2019).

> *(6) Things do not look up for the HiBit reporter assay. The two sequences clearly have effects on translation without considering stop codon context (Figure 4C), which need to be taken into account. Also, the effect from the sequences varies in the context of the assay in 4C and 4D (2-fold vs. 5-fold), further questioning the assay. Moreover, the authors claim that re-initiation cannot account for Hibit levels, but that is clearly incorrect. The western in Figure 4E does not reproduce the data in 4D. While Hibit goes up (as in 4D, the putative GFP-fusion goes down. Finally, while the second reading frame should be more efficient, it is not explained and further argues for an artifact. Previous work (and work herein) suggests that read-through occurs equally in each reading frame.*

The Reviewer is confused about the HiBiT-based reporter assay shown in Figure 4C-4E. First, we have included important controls, i.e., same reporters without stop codons, to normalize sequence variation. Second, Figure 4C and 4D used totally different reporters and it is not appropriate to directly compare their values. Third, re-initiation events would not generate fusion proteins containing the N-terminal GFP. The Reviewer is encouraged to re-examine the results presented in Figure 4.

> *(7) No controls for these assays are presented: e.g., stimulation by antibiotics, ABCE1 depletion, etc.*

We are not sure which assay the Reviewer is referring to. For reporter assays shown in Figure 4, we focused on effects of *cis*-sequence elements, rather than *trans*-acting factors. We thank the Reviewer for understanding.

> *(8) Figure 5 has similar problems. I don't understand how Figure 5A is made, but when one overlays the cited structures on Rps26, the molecules are identical. I guess the authors chose to build non-existing sequences differently into the structure. There is no basis for that. In panel C, and the same in Figure 7, the number of analyzed mRNAs varies. This could influence the outcome, and the EXACT same set of mRNAs should be analyzed. But the main problem here is that the authors need to analyze readthrough*

> *and not peak height, as detailed above. Essential controls are missing that show what fraction of the 18S rRNA is mutated. Previous work has shown that 2 nt-truncated 18S rRNA is actively degraded. It is hard to believe how 15% of altered ribosomes can abolish 100% of the effect from the C-rich sequences. Important validation is missing: the authors should analyze rRNA sequences in their ribo-seq dataset to demonstrate that they have the mutated rRNAs, and that these enrich and de-enrich as predicted.*

The Reviewer's comment on Figure 5A is baseless. As indicated in the Figure legend, Figure 5A was made from the existing cryoEM structure (PDB: 6ZMW). Regarding 18S rRNA mutants, we simply followed prior studies (Burman and Mauro. NAR 2012) and there is no evidence indicating degradation of such rRNA mutants. Given the low percentage of ribosomes incorporated with the rRNA mutants, the observed effect on termination pausing represent an underestimation, rather than an overstatement.

> *(9) In Figures 5-7, the authors develop a model that the sequence selectivity arises from base pairing between 18S rRNA and the mRNA. If so, then they should really stratify the data by the number of WC pairs that can be formed. And only WC pairs, as GU pairs have a totally different geometry that will likely be discriminated against in this context. Also, the mutation is in a part of the helix that has no effect (Figure S3G). Thus, the data within the manuscript are inconsistent.*

As the Reviewer might be aware, GU pairs are commonly found in tRNA and rRNA structures. Since both WC and GU pairs contribute to mRNA:rRNA interaction, there is no point to stratify sequences based on different pairing format. Additionally, we would like to point out that the putative mRNA:rRNA interaction is not static, considering the continuous movement of mRNA along the ribosome channel.

> *(10) Figure 6 does not agree with published data (Li et al., Nature 2022). Previous work did not show testis depletion of Rps26 in purified ribosomes. This is the critical difference, as the authors here did not purify ribosomes. Also, another Rps is an essential control, even if purified ribosomes are used. This dataset should not be shared. Depletion from polysomes is hard to believe, as overall, there is less signal in the polysomes.*

The Reviewer finally made a good point regarding Rps26 in testis. In our study, we did not separate different cell types such as spermatocytes and therefore we do not know which cell type dominantly influences termination pausing.

Regarding varied Rps26 levels in different tissues, we noticed different polysome between testis and liver. Because the polysome volume is difficult to normalize, we used RACK1, a constitutive component of ribosome, to quantify the amount of polysome.

> *(11) Figure 7 has similar problems to Figure 5. Different pools of mRNAs are analyzed; peak height is not validated. Overexpression of Rps26 is not shown, as only Myc is shown, not Rps26. Beyond that, increased occupancy in ribosomes needs to be shown for the effect to come from ribosomes. Given how sick the cells are, it is most likely that all effects are secondary and arise from whatever else is going on in the overexpression or depletion of Rps26. No controls are presented to show specific effects from Rps26.*

We are surprised that the Reviewer ignored the supplementary data that shows Rps26 levels. Regarding controls, it is not appropriate to use different ribosomal proteins because every ribosomal protein has its won functionality. We acknowledge that experiments by gene knockdown is not perfect, but the results are still informative especially when different mRNA pools from the same cells are compared.

> *(11) The authors need to check Rli1/ABCE levels in their cells. Their data have features that are indicative of low ABCE1 levels. These include a very small effect from ABCE1 depletion. These could be responsible for some of the effects they observe.*

Once again, we are surprised that the Reviewer ignored the supplementary data that already shows ABCE1 levels in cells with or without ABCE1 knockdown (Figure S4A). Constantly addressing the Reviewer's lack of careful reading of our manuscript is frustrateing. Nevertheless, we have thoroughly revised the entire manuscript by clarifying interpretations, moderating mechanistic claims, and expanding relevant discussion.

https://doi.org/10.7554/eLife.109257.2.sa0